6-1-1971

Tone Reproduction of Small-Scale Images Using Lithographic Film Under Infectious and Noninfectious Developmental Conditions

Julian Lopez

TONE REPRODUCTION OF SMALL-SCALE IMAGES USING LITHOGRAPHIC FILM UNDER INFECTIOUS AND NONINFECTIOUS DEVELOPMENTAL CONDITIONS

BY

JULIAN E. LOPEZ

Captain U. S. AIR FORCE

Accepted July 28, 1971

H Brent Archer

Ronald Francis

Burt H. Carroll, Advisor

ACKNOWLEDGEMENT

The author is indebted to Professor B. H. Carroll for his guidance, valuable suggestions, and discussions; to Dr. J. A. C. Yule for his careful reading of the manuscript and his valuable suggestions; to Mr. Brent Archer for his helpful comments and suggestions; to Dr. G. W. Schumann for the gradient meter suggestion and help with microdensitometer operation; to Mr. Harry Osborne of Eastman Kodak Company, who has assisted in preparing this manuscript for publication and to all others who have assisted in completing this project.

ABSTRACT

Photographic Science Thesis
Rochester Institute of Technology - 1971

The tone reproduction curve of small-scale images on KODALITH film developed with KODALITH Super Developer were obtained by microsensitometry using a sinusoidal target of 64 percent modulation as a sensitometric tablet to produce images at spatial frequencies corresponding to screen rulings of 9 to 375 lines/inch. A similar series of exposures was processed with addition of sulfite to the developer to give essentially noninfectious development. Speed and contrast with KODALITH developer increased with spatial frequency; speed increased continuously by a small factor and contrast passed through a maximum (80 percent greater than for large area image) at a spatial frequency between 3/8 and 3 cycles/millimeter then decreased with increasing spatial frequency back to the large image level. The contrast and speed for noninfectious development were essentially independent of spatial frequency. The change in speed and contrast for both the infectious and noninfectious development were relatively independent of exposure level.

TONE REPRODUCTION OF SMALL-SCALE IMAGES USING LITHOGRAPHIC FILM UNDER INFECTIOUS AND NONINFECTIOUS DEVELOPMENTAL CONDITIONS

A thesis presented in partial fulfillment of the requirement for the master of science degree in photographic science and instrumentation at the Rochester Institute of Technology, Rochester, New York.

Advisor: Dr. B. H. Carroll

Date: June 1971

Prepared by: J. E. Lopez

SECTION I

INTRODUCTION

1.1. BACKGROUND

In halftone work, tone graduation is produced by breaking up an image into dots of high density and varying size. Lithographic film is exposed through a halftone screen which superimposes a high-frequency pattern onto the original image. These approximately sinusoidal modulations create pin-point dots with minimum illumination. As the exposure is increased the dots grow larger, join in a checkerboard pattern, and as a maximum, close up into a solid area. Formation of dots from two different exposure levels is shown in Figure 1.1.1.

The dot size depends not only on the exposure, but also on the screen ruling. There is a wide variety of contact and glass halftone screens. Screen rulings from 50 to 200 lines/inch are in common use.

Sharp dots are required for quality halftone work. These dots are obtained when there is a sharp boundary between the opaque and transparent areas of the film.[1] "Lith" or infectious development of high contrast film produces characteristic curves with very-high gammas and almost no toe. These characteristic curves approximate a step function, because no density would be produced below a certain level of exposure, but with an additional small increment maximum density would result. In Figure 1.1-2 a step function and a lith characteristic curve are illustrated.

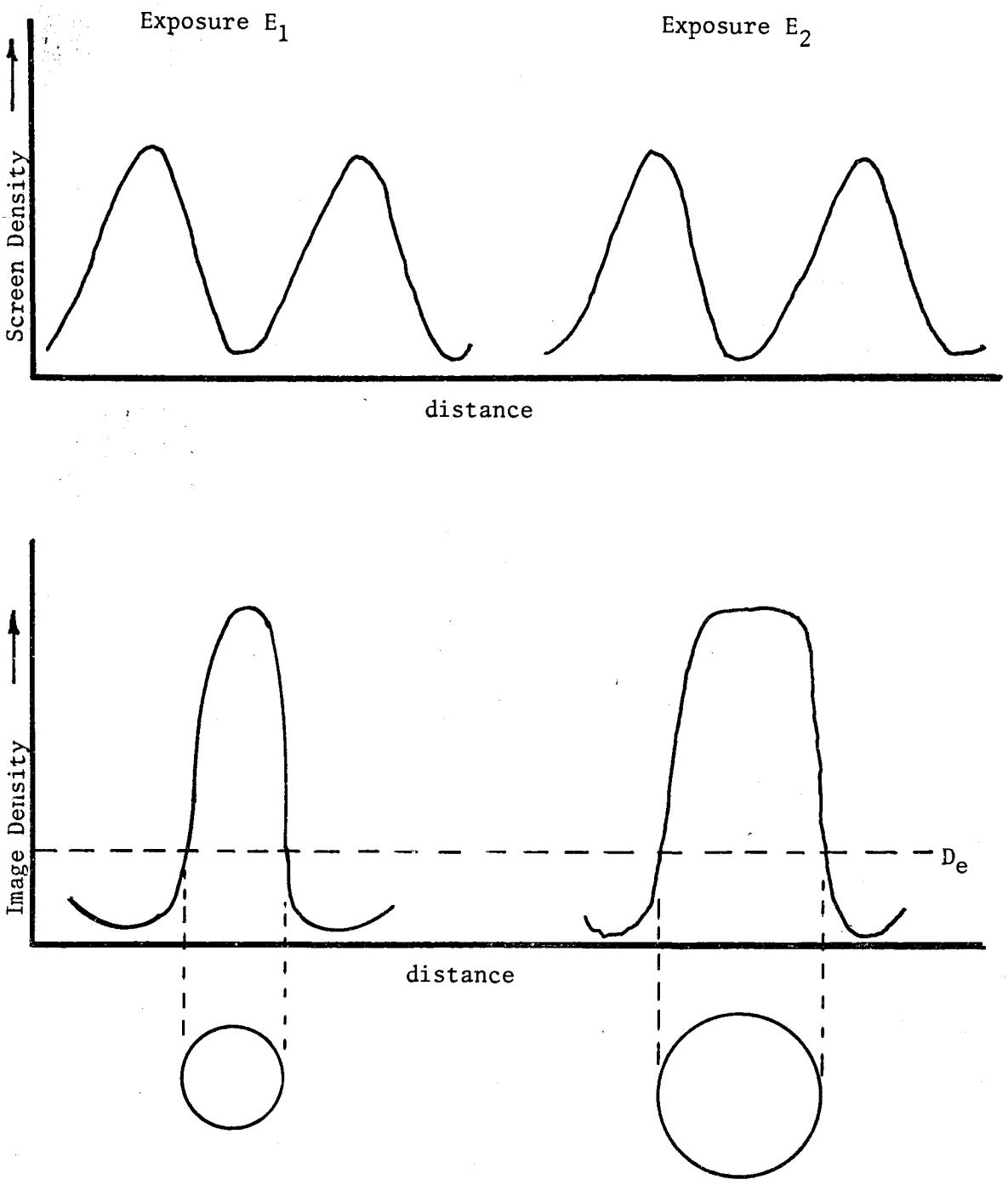

The halftone screen modulates the light so that the dot size (or line width for line screen) increases with exposure.

The size of the dot is measured by the point at which it reaches a specific density $D_e(0.9)$.

FIGURE 1.1-1. DOTS PRODUCED ON LITHOGRAPHIC FILM AT TWO EXPOSURES ($E_2 > E_1$) WHEN EXPOSED THROUGH A CONTACT HALFTONE SCREEN

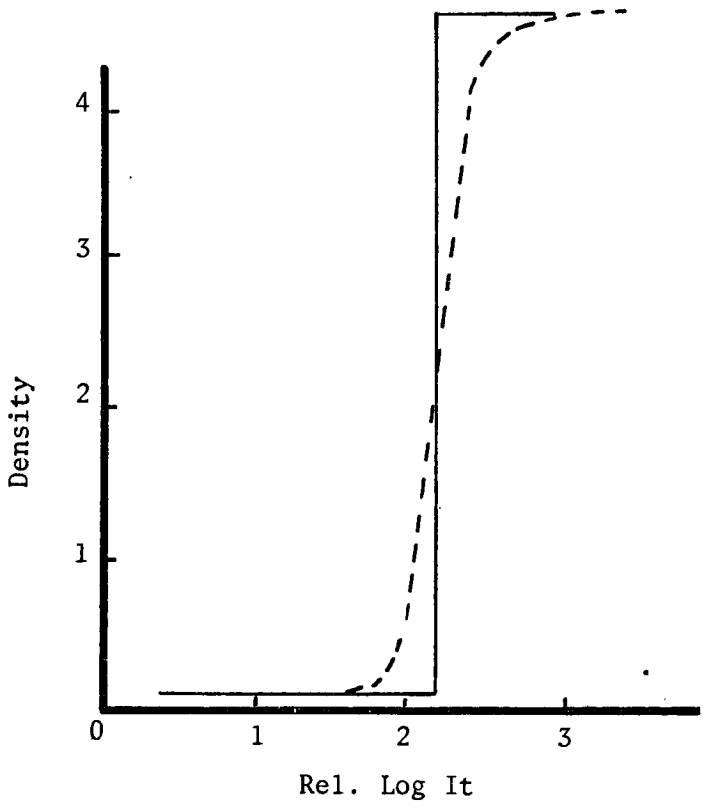

A step function curve _____
and a real "lith" characteristic curve - - - -

FIGURE 1.1-2. AN IDEAL STEP FUNCTION CURVE AND A CHARACTERISTIC CURVE OF A LITHOGRAPHIC FILM

1.2 THEORY OF INFECTIOUS DEVELOPMENT

Infectious development is responsible for the lith characteristic curve. The mechanism for infectious development was based on the reaction of oxidation products of the developing agent, hydroquinone. T, H. James has considered infectious development to come from the reaction of quinone with gelatin to form an active aminohydroquinone.[2] J. A. C. Yule has ascribed infectious development to the reaction of quinone with double charged hydroquinone to form an active semiquinone.[3] Yule's widely accepted mechanism is summarized as follows:

The lith developer contains hydroquinone as the only developer substance. It also contains formaldehyde sodium bisulfite, which by disassociating to a small degree, maintains a low concentration of free sulfite ions. As hydroquinone reduces silver ions, the highly active reducing agent, semiquinone is formed. Quinone, the final oxidation product, and hydroquinone react to form the active semiquinone. Thus once started the reaction proceeds in an autocatalytic manner. The lith developer is most active in the vicinity of developing grains. The intermediate product, which accelerates development, is short lived and its lateral spread is limited by the sulfite in the developer which removes the oxidation products (semiquinone and quinone) as they diffuse outward. Unless an area receives enough exposure to produce a density of about 0.2 the oxidation products will not accumulate to a significant extent and development will proceed with normal activity. With a very small increase of exposure the development products reach a critical concentration and autocatalytic development proceeds. Yule showed that with this type of infectious development only exposed grains are developed.* There is, therefore, a definite density exposure relationship. However, the activity of the developer being strongly dependent on exposure and on the surroundings, one might expect differences between the reporduction curves of large and small scale images. The differences are a form of adjacency effects.

* There are other types of infectious development, such as with hydrazine and its derivatives, which fog unexposed grains.[4]

As in any developer, retarding effects occur because of local exhaustion in the developing agent and local production of halide ions; these adjacency effects are caused by stable materials. However, in lithographic developer there is the accelerating effect resulting from the formation of a short-lived oxidation product (probably semiquinone) which disappears by dismutation and by reaction with sulfite and therefore accelerates development over a relatively short distance.

Quinone has another short-lived oxidation property which can have the interesting effect of accelerating the development of some grains and at the same time destroying the developability of others. In its reaction with hydroquinone, quinone produces semiquinone, the active reducing agent, but at lower exposures and particularly in the presence of bromide, it oxidizes latent-image silver. James in an experiment with a pure bromide emulsion reported that with a quinone solution containing bromide there occurred much less of latent image and a considerable slow down in the rate of development of high exposure areas.[2] Suga working with Lithographic film has shown that latent image bleaching occurred with a quinone pre-bath and to a greater extent with a quinone plus bromide pre-bath. (Effect did not increase with chloride in pre-bath.) The effect was greatest at the lower exposure levels causing a reduction in the toe of the D-Log E curve. The effect increased with the bromide addition or with reduction in the pH solution.[5] In development of a Lith chlorobromide emulsion both accelerating and the latent image bleaching effects may produce significant differences in the small-scale and large-scale images.

1.3 PROJECT OBJECTIVE

It was the purpose of this project to compare the tone reproduction curves of large images produced by standard sensitometry and of small-scale images produced by line screens, both processed with infectious and noninfectious developers and to determine the extent to which lithographic development of halftone images depends on adjacency effects.

SECTION 2

CURVE PRODUCTION

2.1 THE USE OF THE SINUDOIDAL TEST TARGET TO OBTAIN SMALL-SCALE IMAGE D-LOG E CURVES

It was originally intended to use halftone screens with different rulings as sensitometric tablets, with microdensitometer readings of the images, in order to obtain small-scale D-Log E curves. At the suggestion of Mr. Brent Archer a sinusoidal test target with many spatial frequency patterns (see Figure 2.1-1) was used instead. The target had a 64 percent modulation at all frequencies so the density gradient and the distance between lines varied inversely. The use of the sinusoidal test target is similar to the use of a series of screens with the same modulation and varying rulings. As it was not possible, in this project, to separate the effects of distance and density gradient, it would be desirable to make another series of exposures at different modulations giving different density gradients at the same frequency. The modulations of commercial screens is usually higher than that of the sinusoidal test target. This means that for a given spatial frequency the density gradient is larger. For example, a Caprock line screen of 75 lines/inch with a 93 percent modulation has the same density gradient as a spatial frequency pattern of 6.5 cycles/mm (160 lines/inch) on the sinusoidal target. The spatial frequency range selected for study, between 3/8 and 15 cycles/mm (9.5 and 375 lines/inch) covers the practical range of the line screens, both in terms of rulings and density gradient. At these low spatial frequencies the modulation-transfer-function (MTF) of the microdensitometer and the optical spread function of KODALITH film are negligible factors.

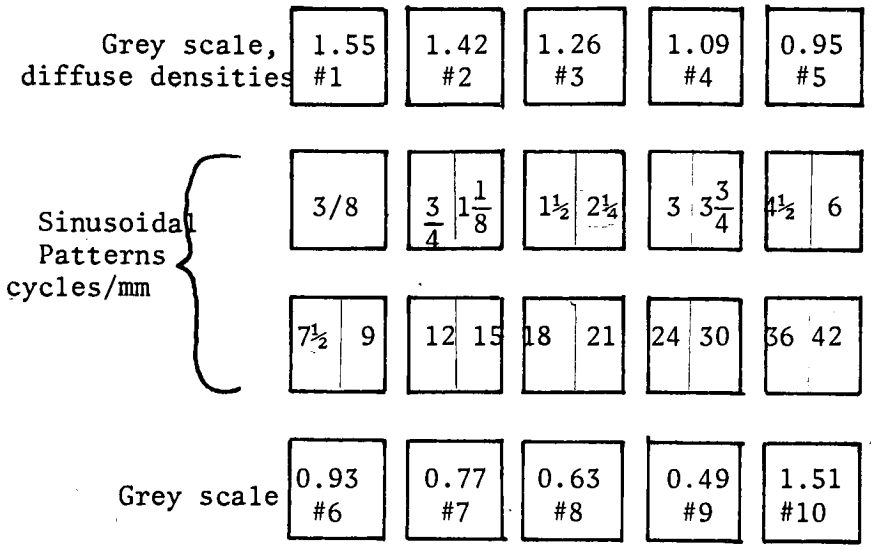

In the above test target the figures for the sinusoidal patterns indicate spatial frequency in cycles/mm; those for the grey scales indicate diffuse density including base plus fog. The numbers for the grey-scale step were assigned left to right. Additional information on this target is found in an article by R.L. Lamberts.[6]

FIGURE 2.1-1. KODAK SINUSOIDAL TEST TARGET OF 64-PERCENT MODULATION

2.2 SMALL-SCALE IMAGE CHARACTERISTIC CURVES

The sinusoidal test target was traced at the selected spatial frequencies with the ANSCO 4 microdensitometer (see Appendix A). The KODALITH images were traced at the same spatial frequencies. For each spatial frequency the microdensitometer traces of the sinusoidal target and of a KODALITH image were matched and dividers were used to find target and image densities that corresponded to each other. Effectively the sinusoidal test target served as a continuous sensitometric wedge in obtaining the characteristic curve (see Figure 2.2-1). Due to the great changes in density that result in the image for a small change in the density of the target, it was decided to select fixed image densities and find corresponding target densities. Normally it would be expected to obtain image densities corresponding to fixed target densities. For further elaboration on this method, its repeatability, etc. see Appendix B.

2.3 LARGE IMAGE-AREA CHARACTERISTIC CURVES

For most films, a large image area characteristic curve can be obtained by using the grey steps of the sinusoidal test target (see Figure 2.1-1) as a step wedge. This was done for the negatives listed in Table 2.4-1. Because of the extreme contrast of KODALITH the curves thus obtained from a single exposure had very few points along their straight-line section (particularly for infectiously developed set). However, exposures were made with four small differences in time, at constant intensity incident on the tablet. Over this range of time or density the recriprocity failure of KODALITH (Figure 2.3-1) is negligible, so the characteristic curves for each time were superimposed by compensating for the difference in Log exposure time. Using this method the resulting infectious and noninfectious curves had sufficient data points along their straight line portion. (See Appendix C) There was good agreement between the curve obtained by this method and by use of a KODAK Type 101 sensitometer.

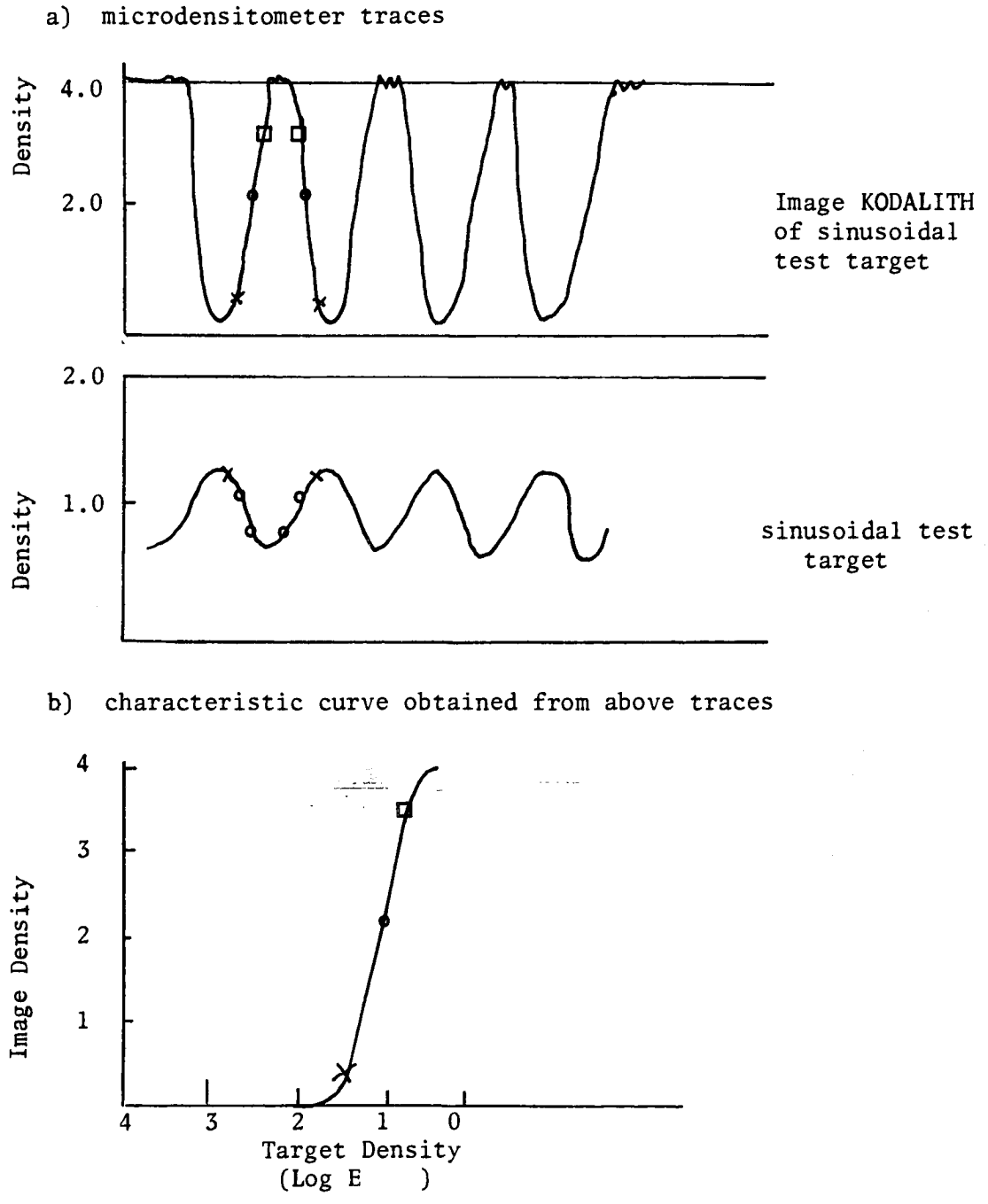

FIGURE 2.2-1. METHOD USED TO OBTAIN CHARACTERISTIC CURVES OF SMALL IMAGES USING DIVIDERS

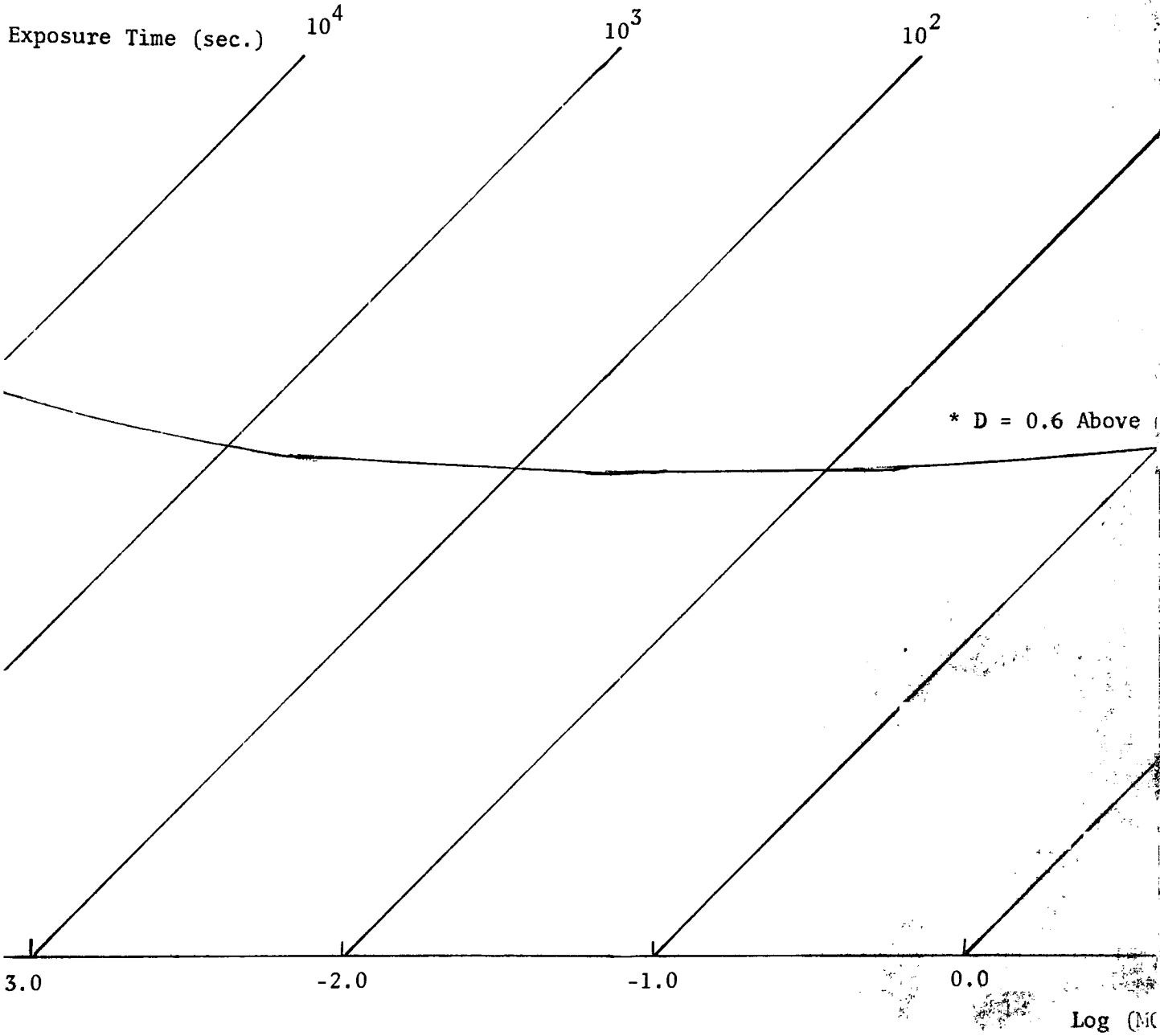

FIGURE 2.3-1. RECIPROCITY FAILURE
WITH KODALITH SUPER

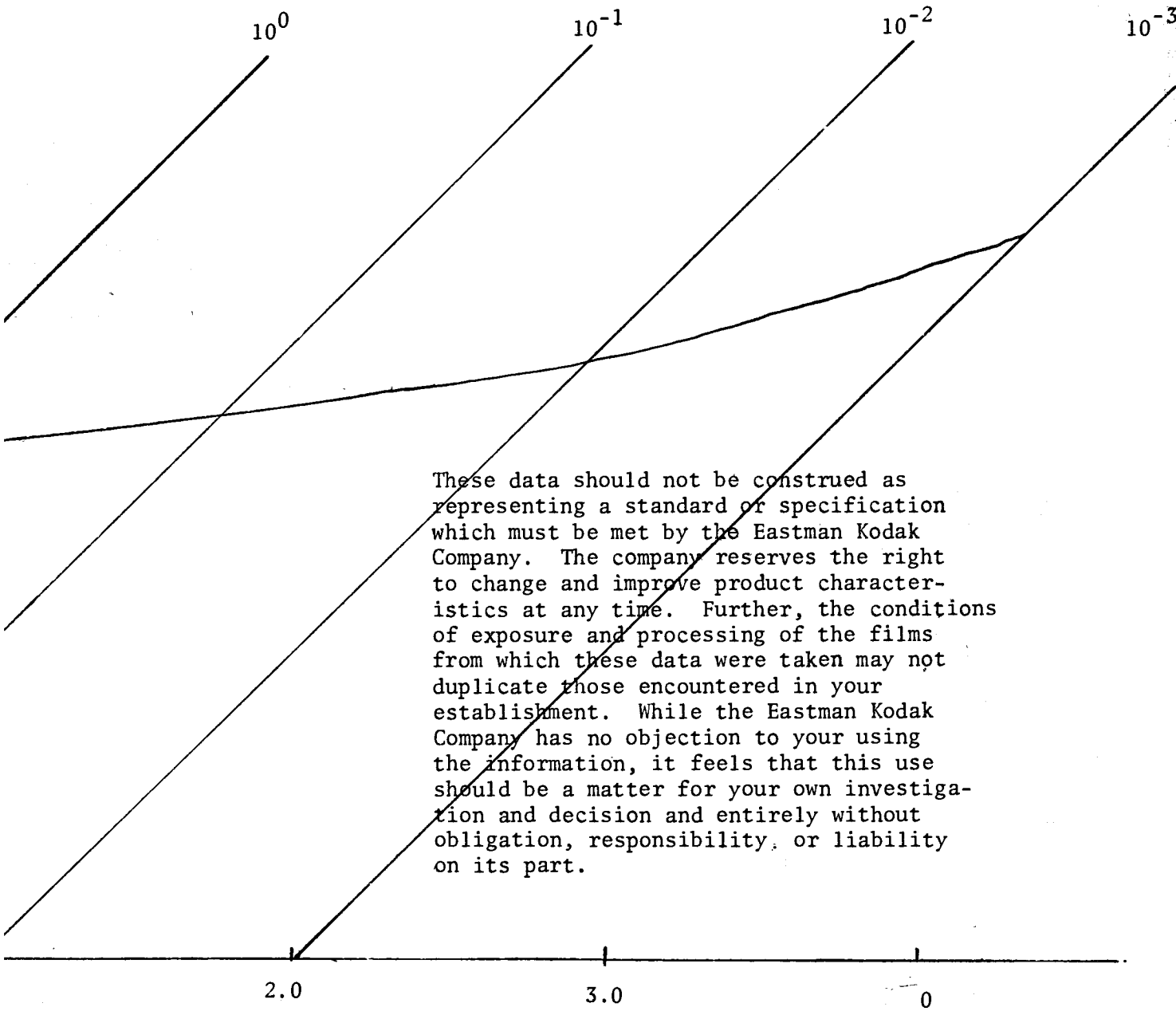

These data should not be construed as representing a standard or specification which must be met by the Eastman Kodak Company. The company reserves the right to change and improve product characteristics at any time. Further, the conditions of exposure and processing of the films from which these data were taken may not duplicate those encountered in your establishment. While the Eastman Kodak Company has no objection to your using the information, it feels that this use should be a matter for your own investigation and decision and entirely without obligation, responsibility, or liability on its part.

KODALITH FILM DEVELOPED
FOR 2 MINUTES 45 SECONDS

2.4 EXPERIMENT

The object was to obtain the characteristic curves for large and small A scale images under infectious and "noninfectious"*conditions; four exposure levels were used to secure enough points on the curve. The KODALITH film was contact exposed through the sinusoidal target (see para. 2.9) the exposure times were 2.5, 3.0, 3.6 and 4.4 seconds. The source intensity was constant. All negatives developed with infectious developer were in one tray, those developed with the noninfectious developer in another (see Table 2.4.1). Development times for both trays was for 2 minutes 45 seconds at 68°F. A study of the effect of development time would be useful, but could not be done in the time available. The sinusoidal target and its images were then traced to obtain the characteristic curves at selected spatial frequencies. These frequencies were 3/8 cycle/mm (9.5 lines/inch), the lowest freqeuncy available, 3, 6, 9, 12 and 15 cycles/mm (75, 150, 225, and 375 lines/inch). These spatial frequencies cover the practical range of line screens, both in terms of rulings and density gradients.

TABLE 2.4-1

KODALITH Images of the Sinusoidal Test Target

Tray 1 (infectious)		Tray 2 ("noninfectious")	
Neg. No.	Exposure time (seconds)**	Neg. No.	Exposure time (seconds)**
65a	2.5**	65w	2.5**
65b	3.0	65x	3.0
65c	3.6	65y	3.6
65d	4.4	65z	3.6 ?

* Quotations around noninfectious indicate that infectious properties were largely but not completely removed, (see para. 2.8).

** At this exposure time the development was insufficient to bring out traceable small-scale images.

2.5 CHARACTERISTIC CURVE PARAMETERS

The sensitivity or speed was measured by the log E required to produce an image density of 0.70 (diffuse). It is expressed as a log value, the target density at the point where the image density is 0.70 for an exposure time of 4.4 seconds. Contrast was expressed as the average gradient, which gives an indication of the sharpness of the line edge. The larger the gradient the sharper the line edge should be. This measurement was made with a gradient meter (see Figure 2.5-1) designed by Dr. G. W. Schumann. The meter measures an average gradient between 0.20 above base plug fog and the point at which the characteristic curve crosses on the gradient meter. The gradient meter is a transparency of an ellipse which was marked at the points where lines of given slopes intersect it. More detail on the gradient meter is given in Appendix E.

2.6 MICRODENSITOMETER VS. DIFFUSE DENSITY

The densities of the small-scale images were necessarily measured with the microdensitometer, which reads semi-specular densities. Interconversion between these and diffuse densities was secured by measuring the images of the step tablet with both the microdensitometer and a Macbeth densitometer (Model TD102) reading diffuse densities; the results are shown in Figure 2.6-1. The extreme contrast of the KODALITH exaggerates the light irregularities of the step tablet, causing the scatter of points. For confirmation, similar measurements were made on another fine-grained film, KODAK SO278, which gave a ratio of 0.82 to 1.0. The data in Figure 2.6-1 are for infectious development; it can be assumed that they can be applied also to noninfectious development of film.

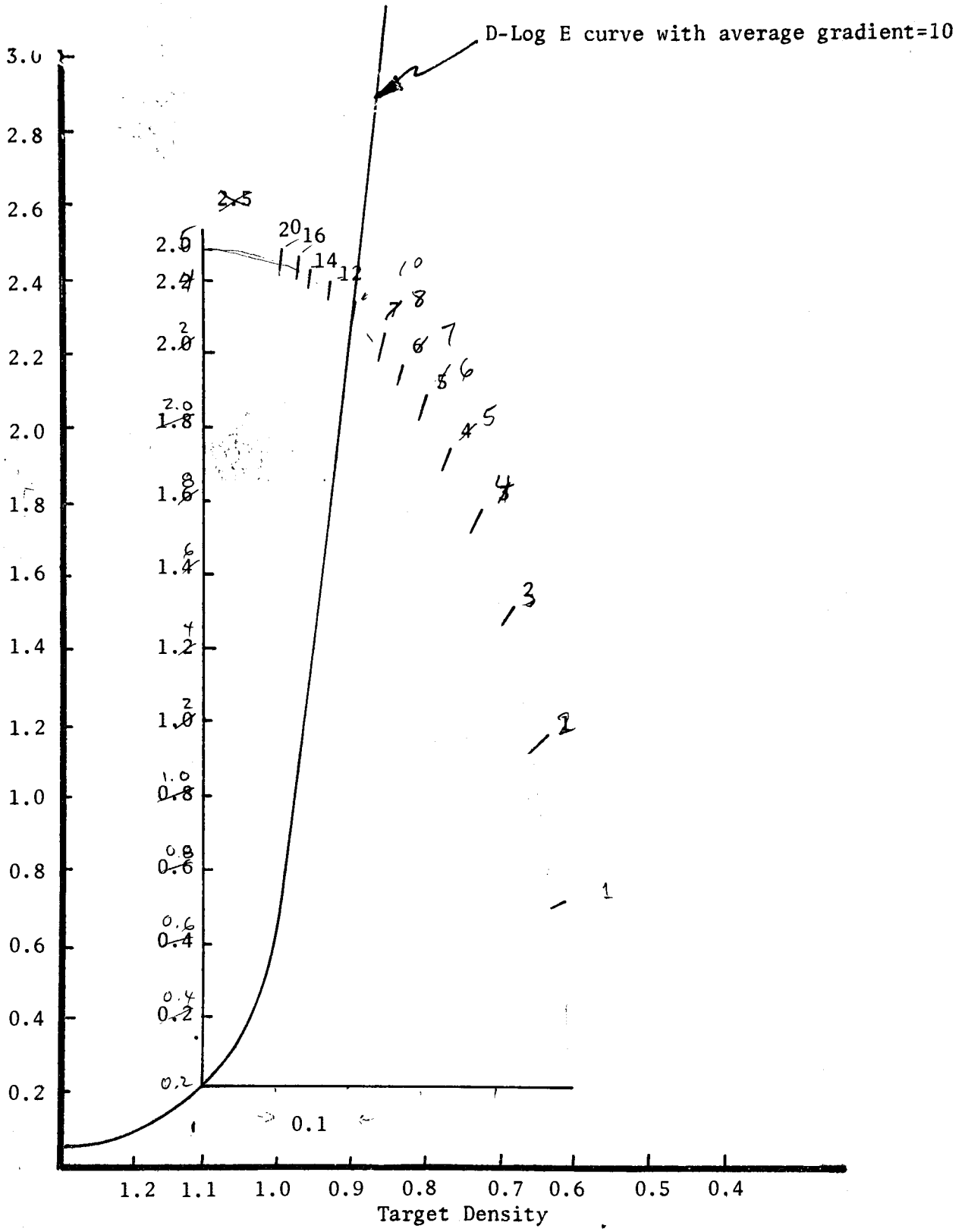

FIGURE 2.5-1. GRADIENT METER USED TO OBTAIN AVERAGE GRADIENTS OF D-LOG E CURVES

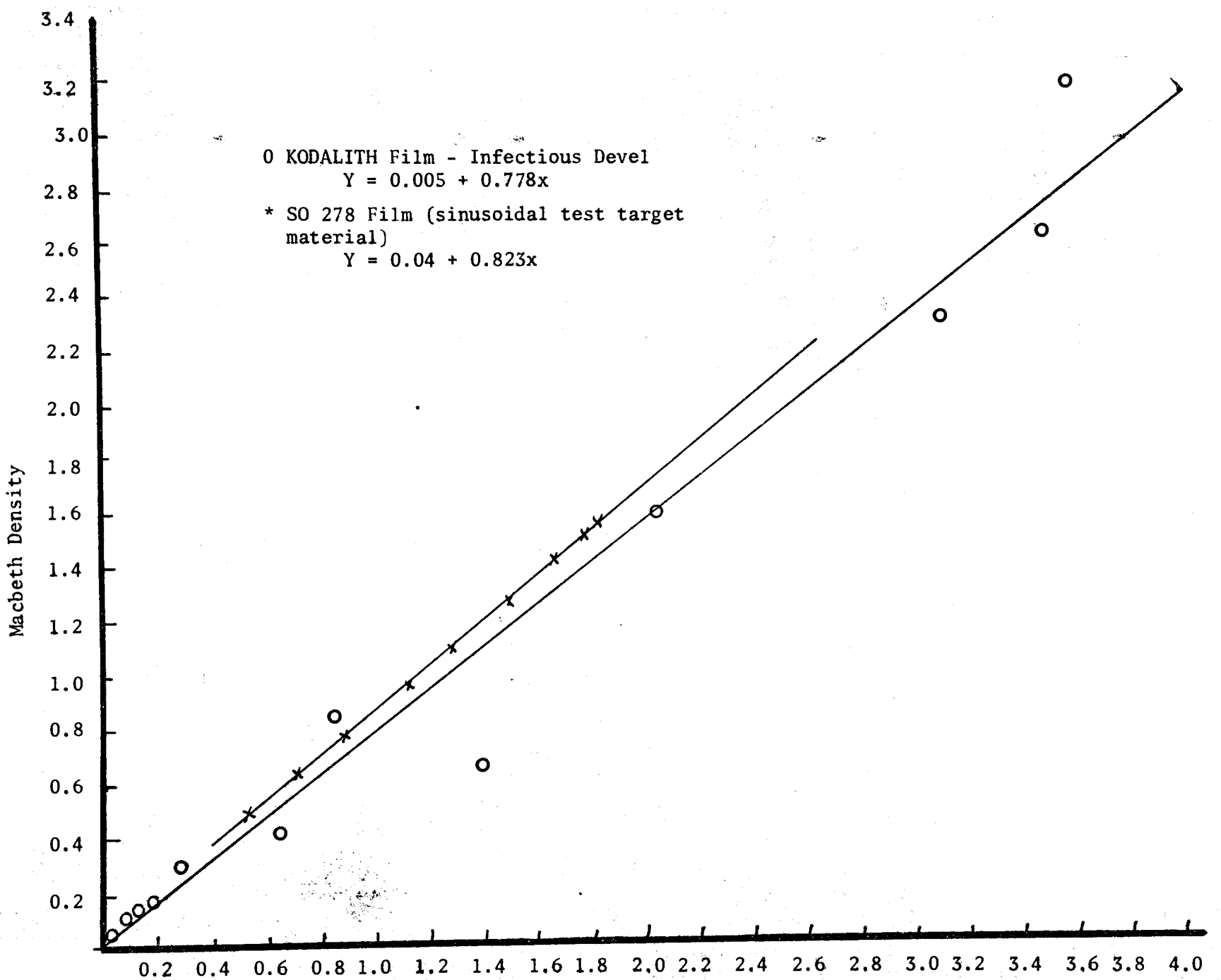

FIGURE 7.6-1. MACBETH VS MICRODENSITOMETER DENSITY

2.7 LARGE-AREA CHARACTERISTIC CURVE DENSITIES

With KODALITH film there are large density changes with small exposure changes. An initial part of this project was producing a step wedge of 0.05 density increments from KODAK High Resolution Film SO 342. It was hoped to obtain large area image D-Log E curves with it, but the images produced from it were of very poor quality. This was due primarily to the high contrasts of both the fine grain KODAK Type SO 342 and KODALITH films, which reproduce an unevenness in the exposure of the step wedge at an overall gamma of about 50. Instead the 21-step Kodak photographic step tablet No. 2 in the 101 sensitimeter and the grey steps of the Kodak sinusoidal test target were used (see para. 2.3) when it was decided the density variations would not have a serious effect. There were uneveness in the exposure of the step wedges that manifested themselves on the images, but in plotting the large area image characteristic curves from two sources the agreement was reasonable. For example, the data obtained from test strips exposed in a 101 sensitometer and from the grey scales of the sinusoidal target produce D-Log E curves that when superimposed are essentially the same (see Figure 2.7-1). With the small scale images the problem of density variations was less pronounced and as seen in Appendix B the repeatability obtained was good. There were apparently two factors in this favorable result, - processing variation over the area of the small images was small, and there was considerable smoothing of small irregularities by the scanning process in the microdensitometer.

FIGURE 2.7-1. INFECTIOUS DEVELOPMENT OF KODALITH FILM-2 MIN 45 SEC 68F

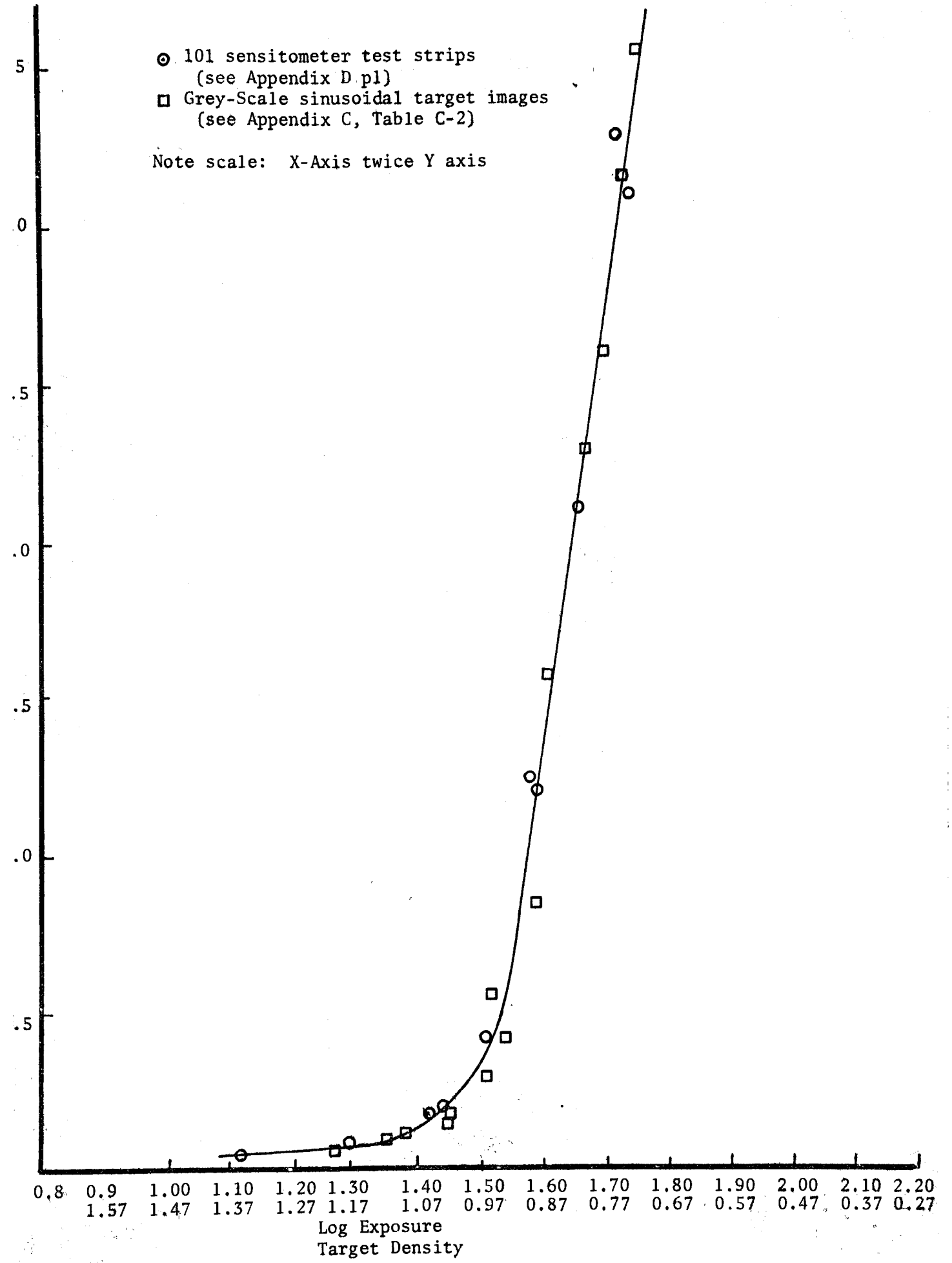

2.8 INFECTIOUS AND "NONINFECTIOUS DEVELOPER

The infectious developer was KODALITH Super developer. The"noninfectious" developer was the same developer plus 20 gm/liter of sodium sulfite. The characteristic curves for the KODALITH Super developer, for the developer with 50 gm/liter of sodium sulfite and for the developer with 20 gm/liter of sodium sulfite were obtained by developing test strips of KODALITH film exposed through a step wedge in a 101 sensitometer (see Figure 2.8-1). All test strips were developed for 2 minutes 45 seconds at 68°F. The D-Log E curve for the KODALITH Super developer had a high gamma and little toe. With sulfite added the characteristic curves had lower gammas, more toe, and higher toe speeds. The lower gamma indicates that the infectious property was removed to a considerable extent. The fact that the gradient of the developer with 20 gm/liter sulfite added is about 30 percent greater than that with 50 gm/liter probably indicates that its infectious property was removed to a lesser extent and that there is increased solvent action of 50 g sulfite on the fine-grained chlorobromide emulsion. The increased toe speeds with "noninfectious" developer is probably due to an increase in the ionic strength (an increase of 1.18 with addition of 50 gm/liter Na_2SO_3 or 0.48 with 20 gm/liter of Na_2SO_3) since pure hydroquinone developers are sensitive to ionic strength.[7,8] There could be a small effect due to increased pH (from 9.91 to 9.94 with 20 gm/liter of Na_2SO_3). The developer with 20 gm/liter of sodium sulfite was chosen as the "noninfectious" developer for this project in order to minimize the solvent action which sulfite has on silver halide.

FIGURE 2.8-1. INFECTIOUS AND NONINFECTIOUS DEVELOPMENT OF KODALITH FILM

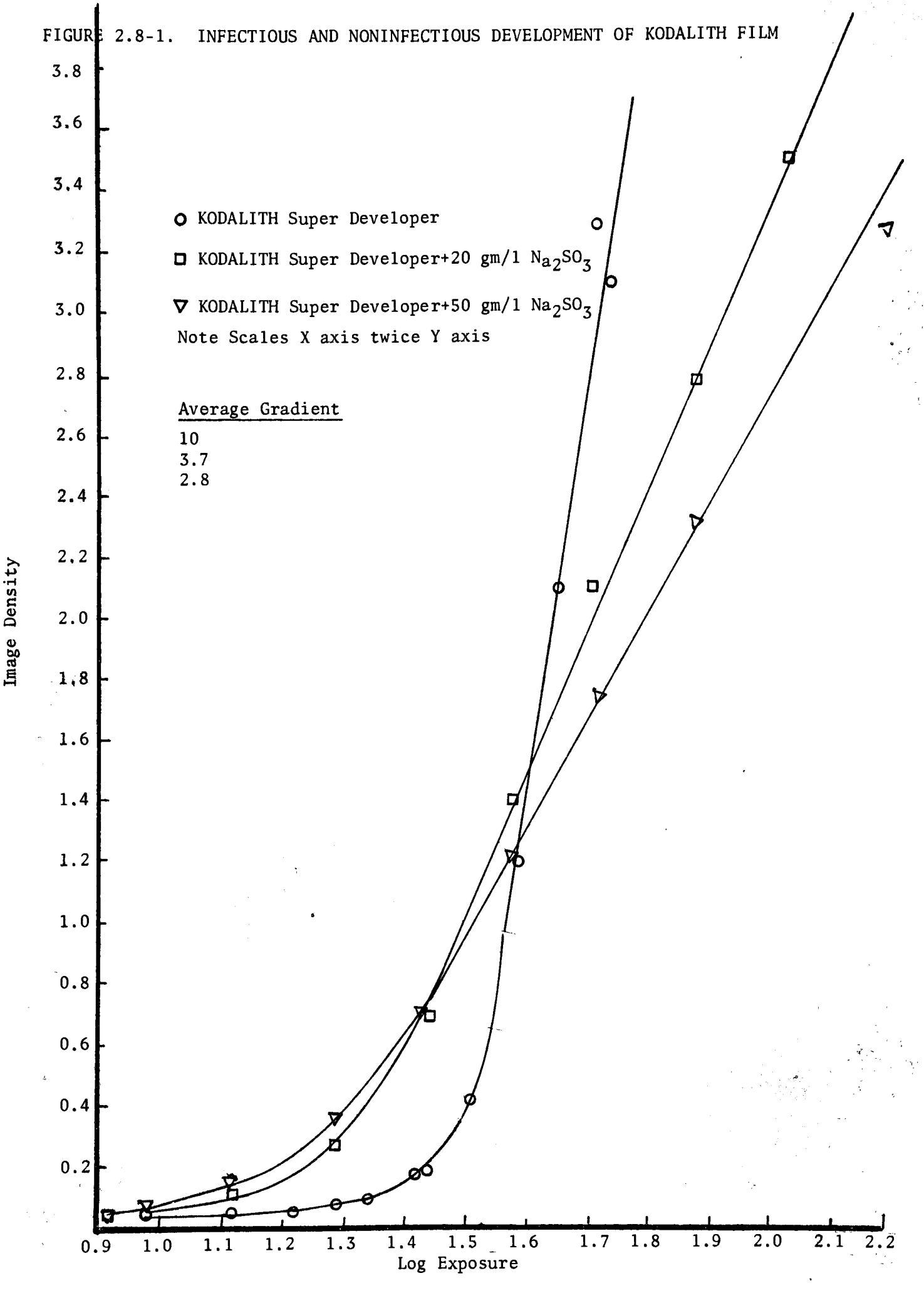

2.9 EXPOSURE USING THE KLIMSCH VAKUMATIC MACHINE

A Klimsch Vakumatic machine was used to expose the KODALITH film to the sine-wave target (see Figure 2.9-1). The Kodak target was placed on the glass surface, the film (emulsion side down) was placed over the target and then the vacuum cover was closed. Xylene was used as a contact liquid between the glass and target and between the target and film. Without Xylene, very bad Newton rings were formed. A rotating tungsten bulb was used to make the exposure. The rotating bulb was designed to ensure uniform illumination throughout the glass surface of the Klimsch Vakumatic machine. The red safe light actually contributed to the exposure. Alone, this red bulb has no measurable effect but with additional fogging exposure plus an exposure through the sinusoidal test target significant variations in density were obtained. When this was discovered, negatives handled and exposed while this bulb was on had to be discarded.

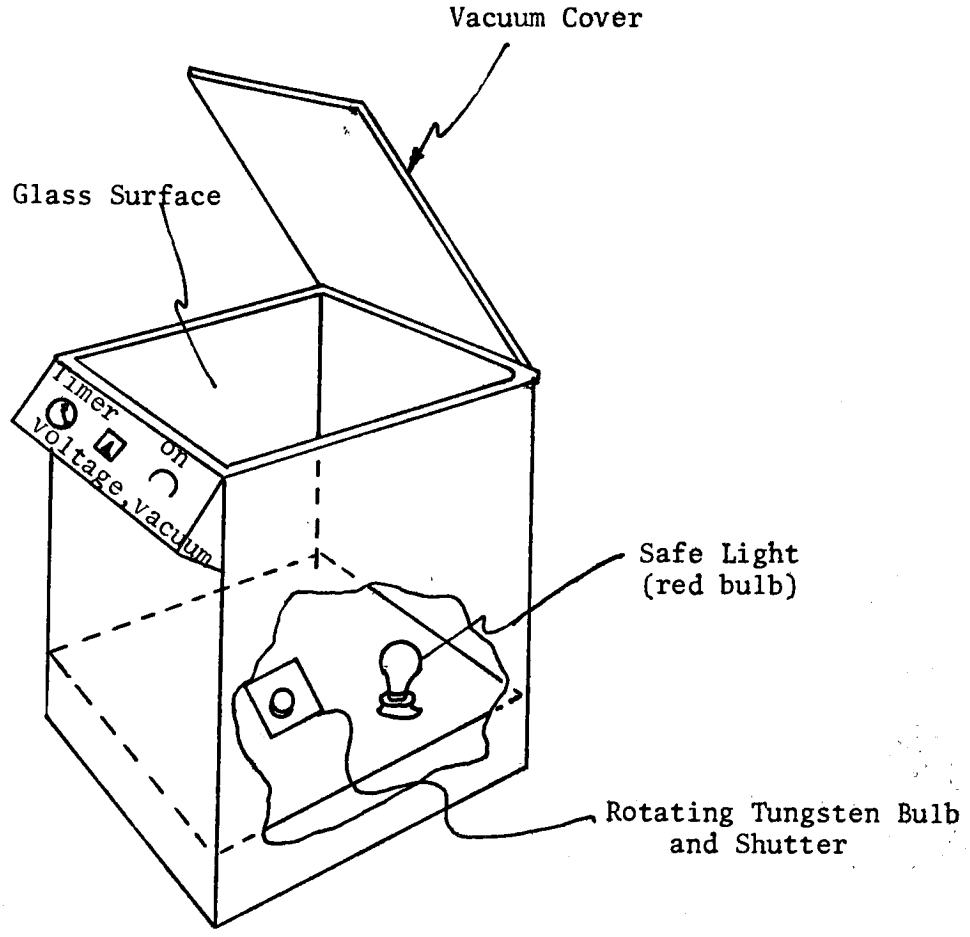

This machine has a small rotating bulb and a shutter. The source intensity is controlled by the voltage which was set at 7.5 volts.

FIGURE 2.9-1. KLIMPSCH VAKURNATIC MACHINE USED TO MAKE EXPOSURES

SECTION 3

RESULTS

3.1 INFECTIOUS DEVELOPMENT

KODALITH images of the sinusoidal test target produced at three exposure levels (see Table 2.4-1) were used to obtain the large image (see para. 2.3) and the small scale image D-Log E curves (see para. 2.2). Negative 65d is the KODALITH image at 4.4 seconds exposure time. Four of the curves derived from this negative are reproduced in Figure 3.1-1. This same pattern was obtained at the other exposure levels and frequencies. The summarized results for speed are presented in Figure 3.1-2A and for gradients in Figure 3.1-3A. The small scale images have significantly higher contrast in the frequency range common in halftone practice, the improvement over large scale reproduction reaching a maximum somewhere between 3/8 and 3 cycles/mm (9.5 and 75 lines/inch). At frequencies above 3 cycles/mm the contrast falls ~~(with increasing frequencies above 3 cycles/mm contrast falls)~~ with increasing frequency, reaching that of the large image curve at about 10 cycles/mm. As there is no reciprocity failure (see Figure 2.3-1) over the range of exposure times used, the speeds at 0.70 image density for all the negatives were normalized and compared. There was no significant difference in the speed vs spatial frequency relationship at the different exposure levels, that is, the increase in speed with spatial frequency was similar for the three exposure levels tested. The average of the normalized speeds at each spatial frequency was plotted (se Figure 3.1-2A) and a regression of the values made. The regression (large area image excluded) indicated that the speed vs spatial frequency linear term was real or that there was a real change in the sensitivity. The change in the sensitivity expressed in log units is not large. However, because of that change difference in density produced from a given exposure at the different spatial frequencies can be very large (see Table 3.1-1).

TABLE 3.1-1

VARIATION OF IMAGE DENSITY W/SPATIAL FREQUENCY

FOR

NEG 65d FOR A TARGET DENSITY (LOG E) OF 0.90

IMAGE DENSITY	SPATIAL FREQUENCY
0.10	3/8 cycles/mm
0.13	3 " "
0.44	6 " "
0.76	9 " "
0.82	12 " "
0.98	15 " "

The average gradients obtained from the KODALITH Image characteristic curves followed the same pattern at the three exposure levels. No difference in gradient due to exposure level could be shown. The average value at each spatial frequency was therefore obtained and plotted with a plus and minus two standard deviations about the mean. (see Figure 3.1-3A) The highest average gradient occurred at a spatial frequency of less than 3 cycle/mm (75 lines/inch and was 80 percent greater than the large image average gradient. The manner in which the gradient changes with spatial frequency is of interest in halftone reproduction since the higher gradients can be expected to produce the sharpest dots. For the target used spatial frequencies of 3 cycles/mm (75 line/inch) or lower have the optimum average gradient. It is of interest that the gradient at the higher spatial frequencies start to drop below that of the large image. The reason for this is not optical spread, since it is negligible at the relatively low spatial frequencies considered. With the "non-infectious" development the small scale image average gradients never drop below that of the large area image. The change in speed with frequency indicates that there is a change in the percent line width of the image for a given exposure. The increase in the line width is proportional to the antilog of the speed. For dots the effect will be larger, since the dot area is proportional to the line width squared, that is, to the square of the antilog of the speed.

FIGURE 3.1-1. INFECTIOUS D-LOG E FOR SEVERAL SPATIAL FREQUENCIES

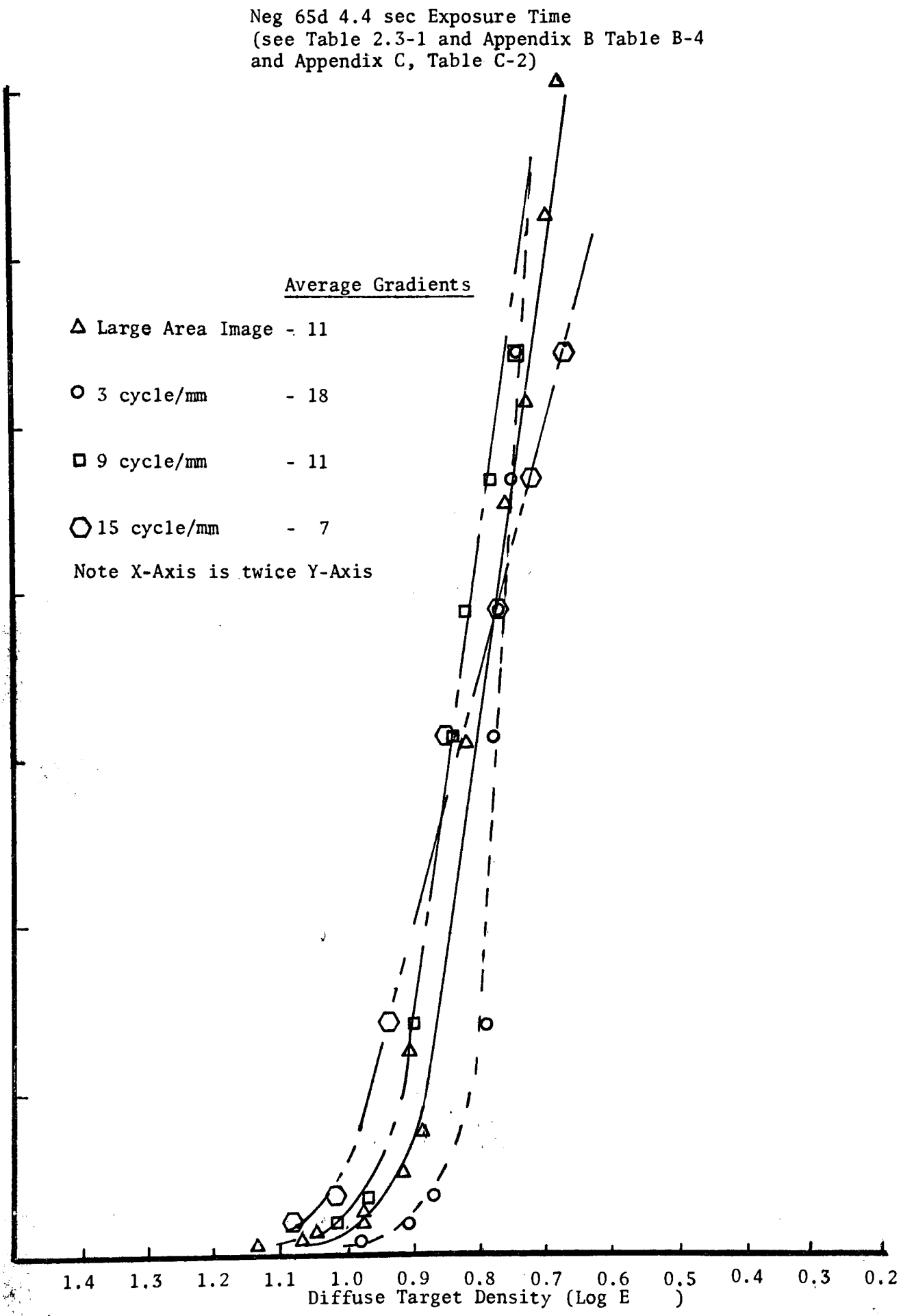

FIGURE 3.1-2 SPEED vs. SPATIAL FREQUENCY (with target density gradients fo r 64% modulation).

A Infectious Development

X = Average from Neg's 65b, 65c & 6
(See Appendix B Table B-4)

$X \pm A_X$ confidence intervals

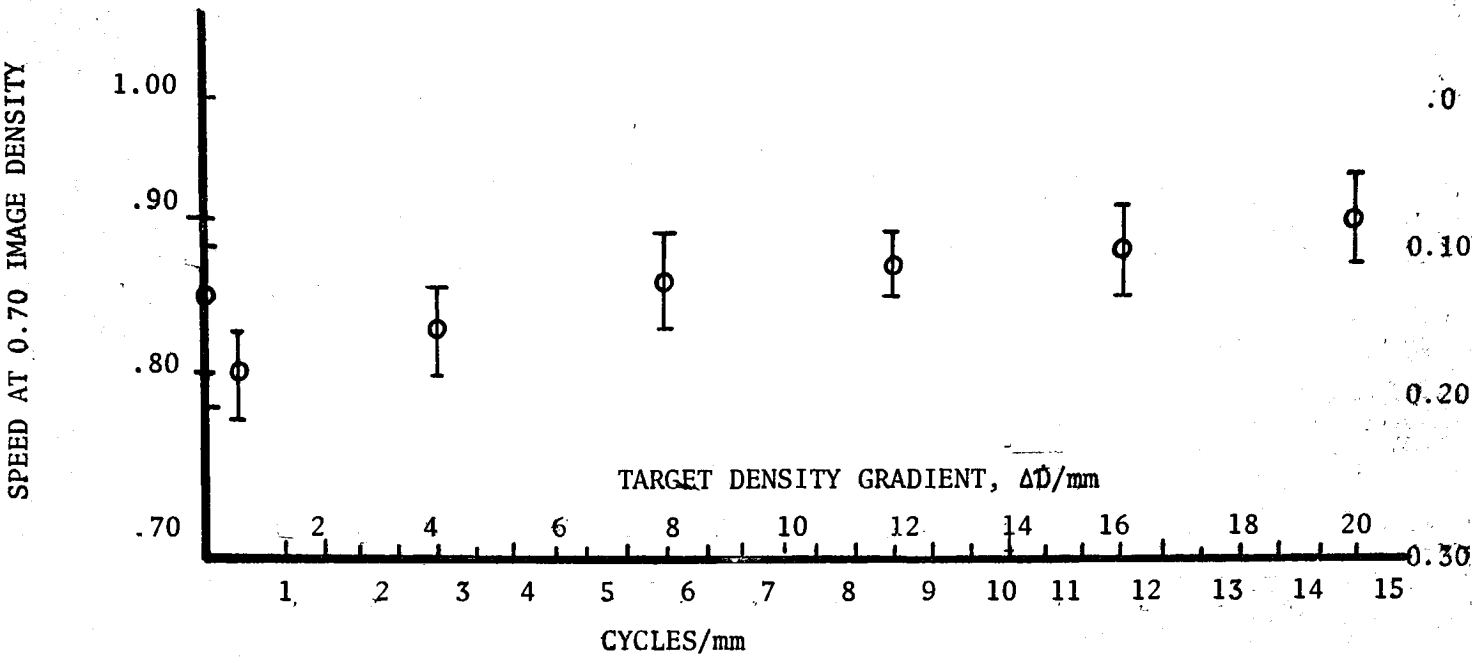

B Noninfectious Development

X = Average from Neg 65x 65y and 65z
(See Appendix B, Table B-5)

$X \pm 2A_X$ confidence intervals

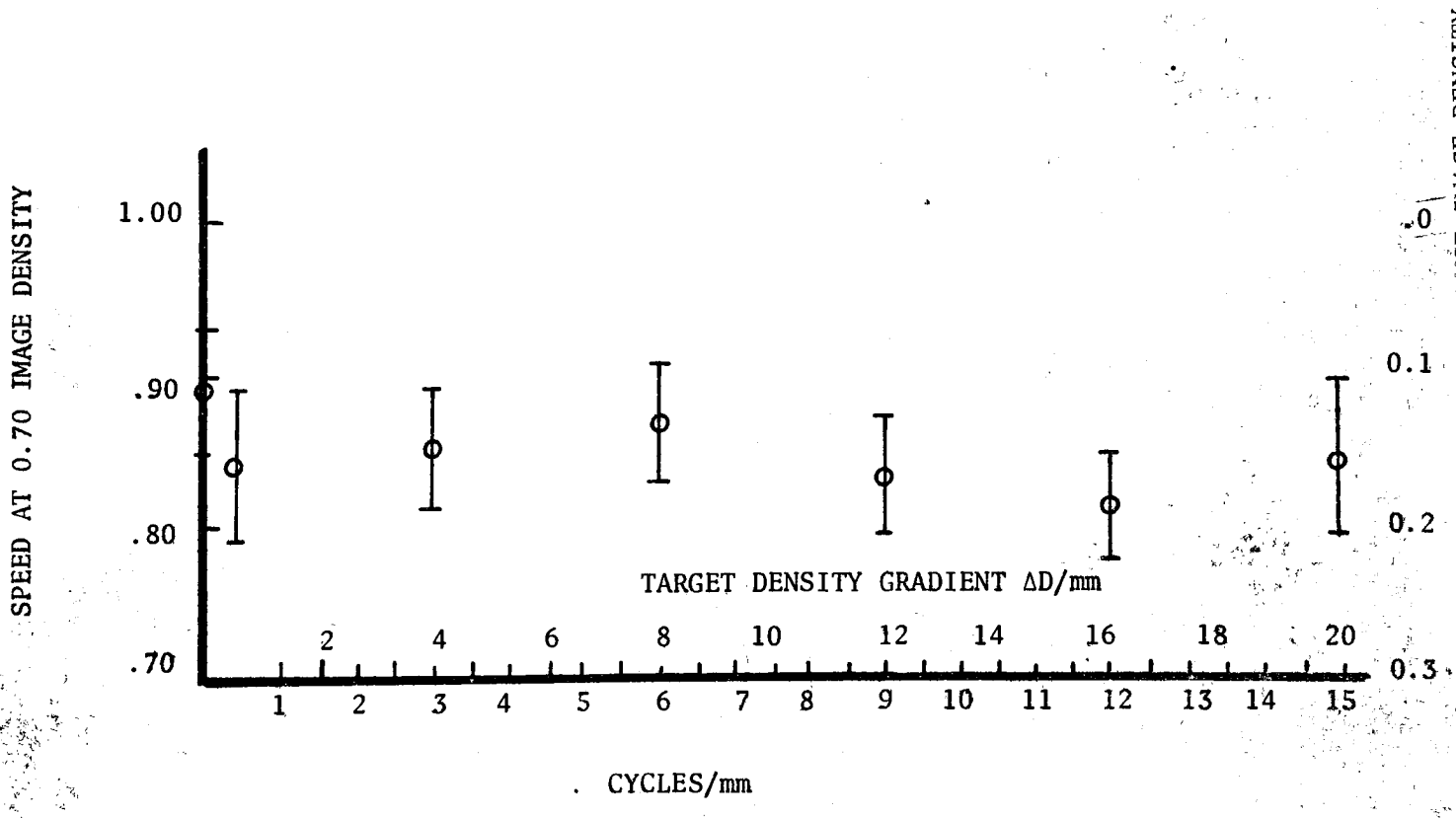

A INFECTIOUS DEVELOPMENT (See Appendix E, Table E-1)

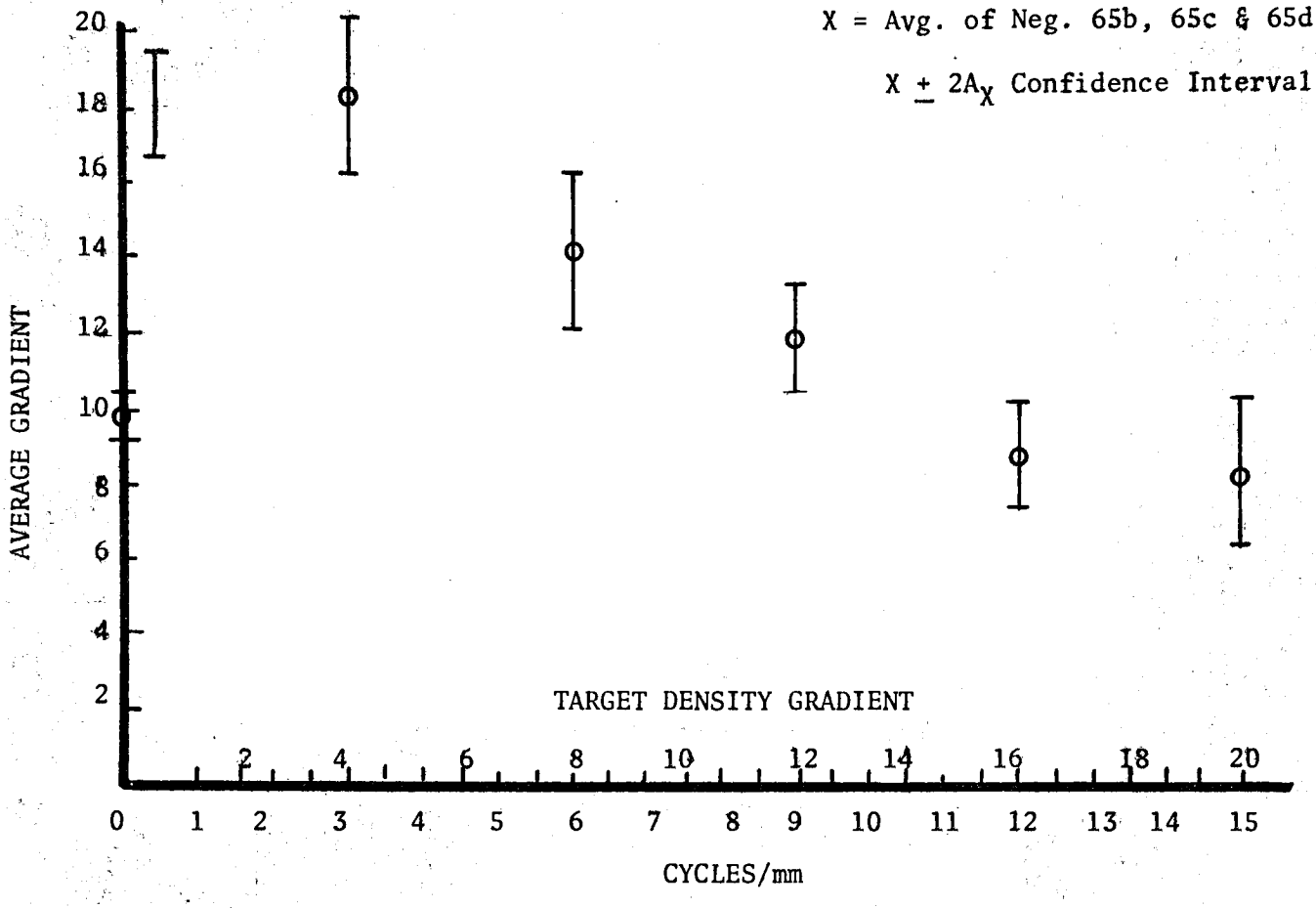

B NONINFECTIOUS DEVELOPMENT (See Appendix E, Table E-2)

Note: Y Scale is twice Y Scale on A

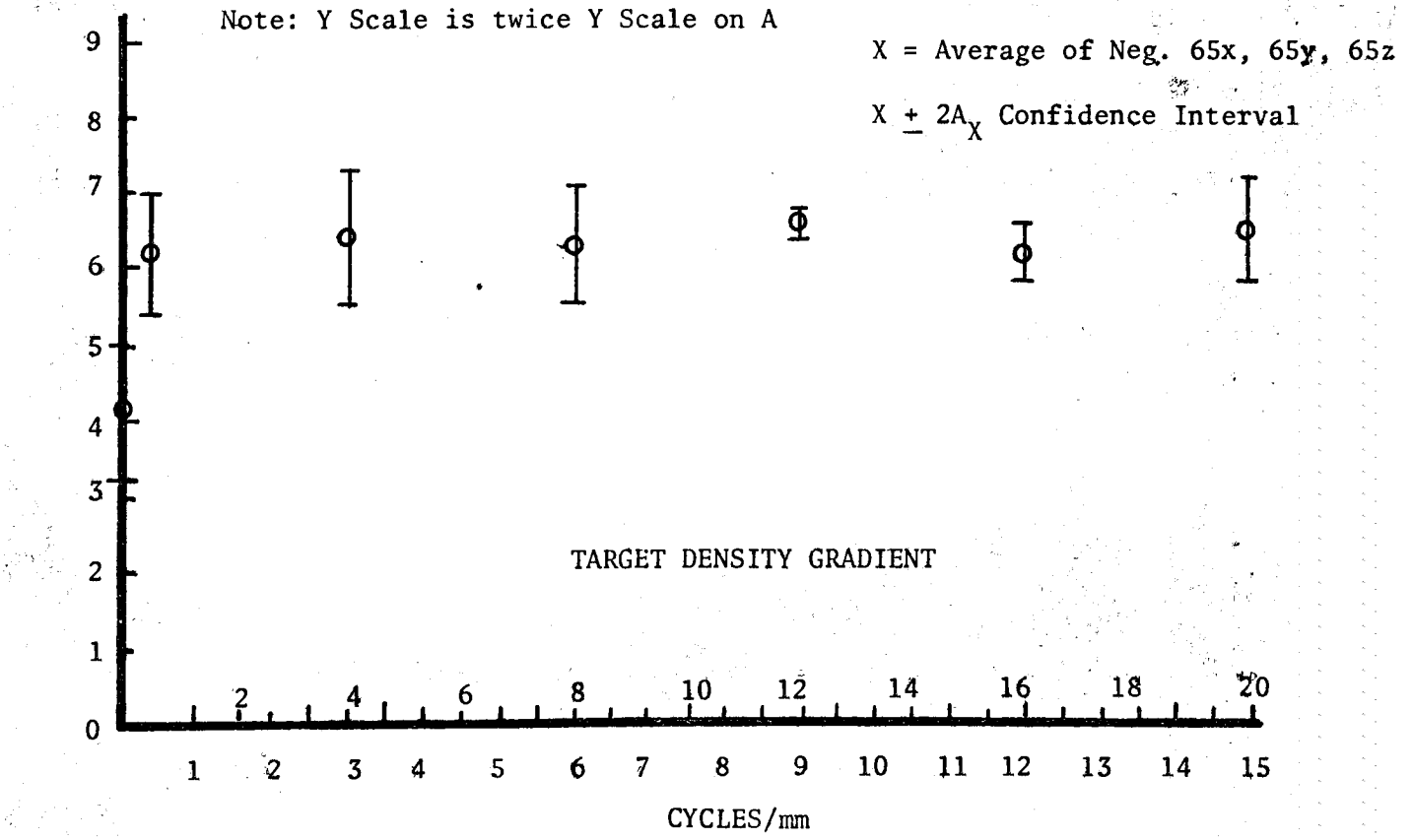

3.2 NONINFECTIOUS DEVELOPMENT

The results for noninfectious development were also obtained from the D-Log E curves. Negative 65z is the KODALITH image at one exposure level. All of the curves from the sine-wave target have slightly lower speed and higher contrast than the large-area curve, but there are no significant changes with frequency among them. Although it is not possible to say that infection was completely eliminated by the addition of sulfite, the differences between the developers can safely be ascribed primarily to infection. The gradients for the small image D-Log E curves vary with no apparent pattern but are different from the large image gradient. (See Figures 3.2-1, 3.1-2B, and 3.1-3B.) The two negatives receiving less exposure showed the same result except that the variability of their speed and gradient measurements were larger. The reason may be that $D_{max.}$ was not reached and that the irregularities found at the peak density of the line being traced contributed to the resulting D-Log E curve.

3.3 INFECTIOUS VS. NONINFECTIOUS DEVELOPMENT

The infectious development results in a different characteristic curve at each of the spatial frequencies tested, that is, speed and gradient are different at each spatial frequency. Noninfectious development produces characteristic curves which are the same (except for random error) for all the small-scale images. The characteristic curves from the large image are different from that of the small-scale images in that their gradient is smaller. Note that the gradient from the small-scale images never falls below that of the large image with noninfectious development, while with infectious development the gradients do start to fall.

FIGURE 3.2-1 "NONINFECTIOUS" D-LOG E FOR SEVERAL SPATIAL FREQUENCIES

NEG. 65z 4.4 SEC. EXPOSURE

(See Table 2.3-1 & Appendix B, Table B-5 & Appendix C, Table C-2)

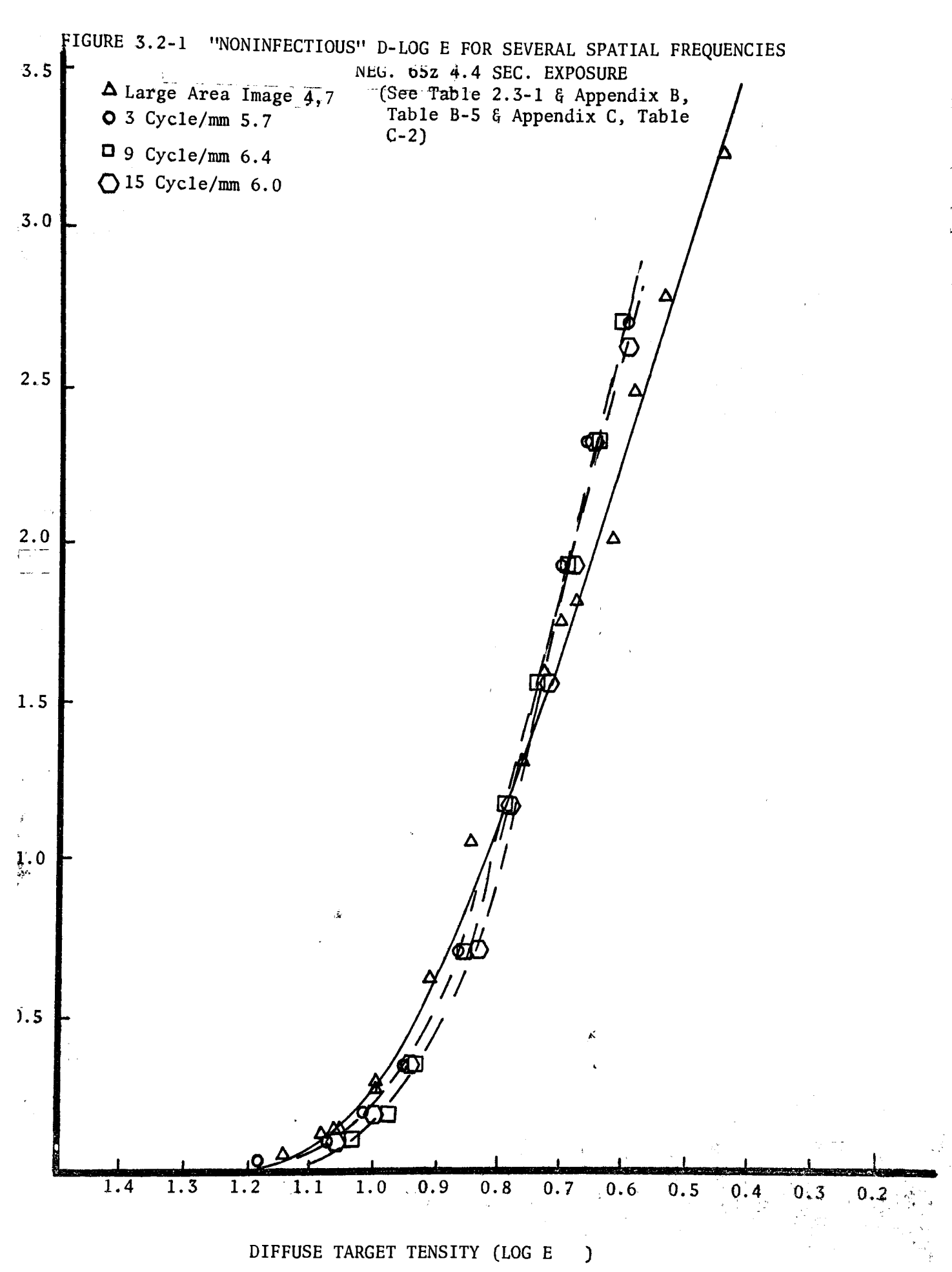

SECTION 4

DISCUSSION

4.1 EXPLANATION OF THE RESULTS

There are several factors which could be responsible for the observed results. These are spatial frequency or the distance between lines, density gradient which is determined by the modulation and frequency, and image size per se, or by a combination of any or all of the above. The separation of the effects will require additional study. The results obtained are applicable to line screens having the same spatial frequency and density-gradient relationships as the sinusoidal test target. The differences in characteristic curves obtained for infectious and noninfectious small-scale and large-area images are to be explained in terms of life times and concentrations of the accelerating and retarding products of development. An explanation for the results is that the accelerating oxidation product has a major effect in the case of the infectious developer and a negligible one with the noninfectious developer. It is assumed that the accelerating product has a short diffusion range. This assumption is made because the product has a short life, being eliminated by dismutation or reaction with sulfite. The retarding products Cl^-, Br^-, H^+) have indefinite life and the reduction of hydroquinone concentration is equivalent to a long-life-time product.

The large-area image has uniform concentrations of developer and developer products, except at the edges. However, for a sinusoidal pattern the development products, semiquinone and halides, diffuse from the high-density areas to the low-density areas. Fresh developer diffuses from the low-density areas to the high-density areas producing additional development and also combining with quinone to form more semiquinone. At a low spatial frequency the small-scale image is relatively large and it has a small density gradient. The large size of the image will give rise to a high concentration of the accelerating product, of the retarding products and perhaps of the quinone which can bleach the latent image at the low-exposure areas. With a short range of accelerating product much diffusion from one high-intensity area to another may occur (see Figure 4.1-1, point A to B).

FIGURE 4.1-1

A Diffusion of Accelerating Product from Point of Formation

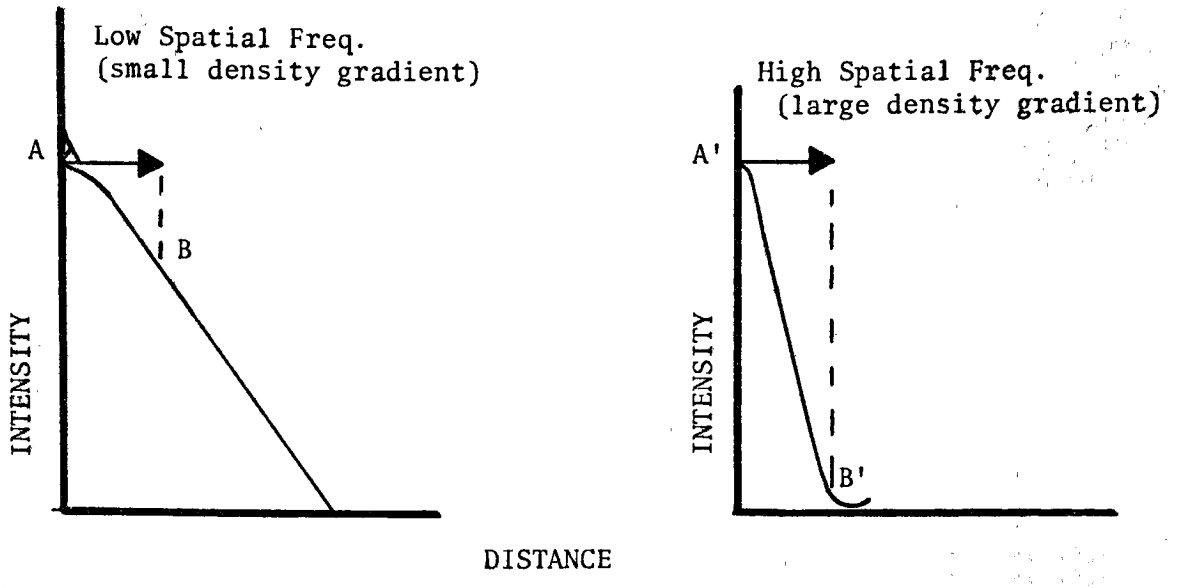

B Developer Activity due to (Cumulative) Accelerating Product and to Accelerating Product minus activity removed by retardants

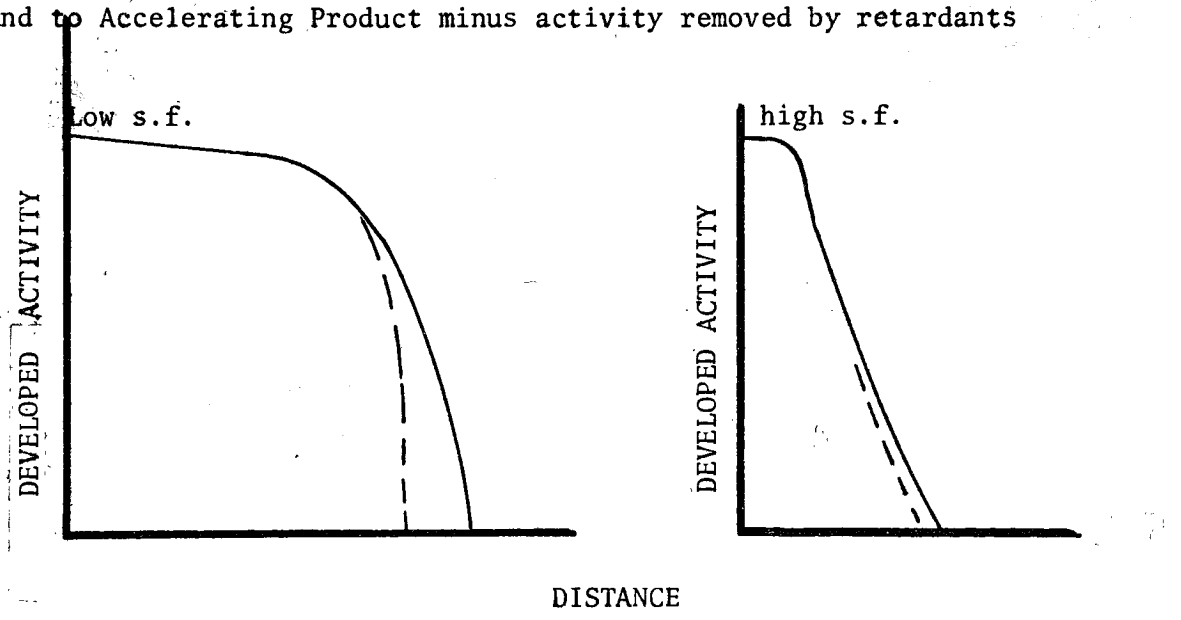

Also the large amounts of retardent products and quinone may result in depressing the density in the areas of low exposure. The end result could be a D-Log E relationship having a high gradient and low speed such as was obtained for the 3 cycle/mm pattern (see Figure 3.1-1). The speed for the 3 cycle/mm pattern was lower than for the large area image. At high spatial frequencies the small-scale image is small and the density gradient is large. The small image will rise to a relatively low concentration of the accelerating and retarding products. The accelerating product with its short diffusion range would move from high-intensity areas to low-intensity areas predominantly (see Figure 4.1-1, point A' to B'). The end result could be more development in the low-exposure areas or more speed, but less development along the line edges or a smaller gradient.

With the noninfectious developer the change in gradient between the large image and the small scale images (see Figure 3.2-1 and 3.1-2B) may be due to the increased solubility of the fine-grained chlorobromide emulsion which results with the addition of sulfite and also to some remaining infectious property. These effects could manifest themselves best with the small scale images.

SECTION 5

CONCLUSIONS

5.1

The tone reproduction of small-scale images obtained using a sinusoidal test target of 64 percent modulation, with microdensitometer measurement of the images and the large-area images obtained by standard sensitometry, for KODALITH Film developed with KODALITH Super Developer (infectious) and with the same developer plus 20 gm/liter sodium sulfite (noninfectious) had contrast and speed relationships which were relatively independent of the exposure levels used. Those used were Log It=2.31, 2.39 and 2.57.

5.2

The tone-reproduction curves obtained for the small-scale images with the infectious developer showed significantly greater contrast than for large areas. The contrast was greatest (80 percent higher than for large-area image) at spatial frequencies between 3/8 and 3 cycles/mm and then decreased with spatial frequency back to the level of the large area image. The speed increased continuously with spatial frequency by a small factor. The speed of the large-area image was between that of the lowest spatial frequency and that of the highest.

5.3

Using the noninfectious developer(KODALITH plus 20 gm/liter of sodium sulfite) contrast and speed were essentially independent of spatial frequency though there was a difference between the small scale and large area curves. Since optical spread is negligible, this result of the noninfectious developer compared with the infectious indicate that the effects are to be explained in terms of accelerating and retarding product concentrations and lifetimes.

BIBLIOGRAPHY

1. Banreusel and Verbrugglie, On Infectious Development, Reprographie Internationaler Kongress, Koln, 1963, p. 91.
2. T. H. James, Photo Science & Engineering 12:67 (1968)
3. J. A. C. Yule, J. Franklin Institute 239 (1945) 221.
4. Stauffer, R. E., Trivelli, A. P. H. and Smith, W. F., J. Franklin Institute, 238 (1945) 291.
5. Suga, Tsuneo, Studies on Lith Development (I) and (II). J. Social Science Photo. Japan Vol. 32 (2), 87-94 (1969) and Vol. 32 (3), 138-43 (1969).
6. R. L. Lamberts, Applied Optics, Vol. 2 No. 3 (1963) 273.
7. Mees and James, Theory of the Photographic Process, 3rd Edition, p. 289.
8. J. S. Levisky, The Inhibition of Aeria Fog, Thesis, RIT, 1969.
9. Kark Frank, Tokyo Conference, 1967 paper III-2.
10. H. M. Cartwright, Illford Graphic Arts Manual, Vol. I 1961.
11. Kodak Graphic Arts Data Book Q-3, Halftone Methods for Graphic Arts.

APPENDIX A

OPERATION OF ANSCO-4 MICRODENSITOMETER

For all traces the slit used was 0.125 by 15 mm (1.2 micron width) on the sample. The magnification was 10/10 for the eyepiece and objective of the reading microscope, 8X for the objective of the source microscope. The instructions provided with the ANSCO-4 microdensitometer were used. The sinusoidal test target and its images were placed in the sample carrier, which was placed over grid paper and rotated until the target images were perpendicular to the direction of the stage movement. Once in the carrier the sample could not be rotated. The microdensitometer was focused on the sample at each frequency pattern. The pre-slit centering knob of the source microscope was checked to ensure that the optical path was clear. The source slit was then closed down to the point that any further closing affected the density. The voltage was then set so that the base plus fog read zero. The next step was to close the slit to the point that a density of 0.1 was indicated on the trace paper. This was done to trace the narrow lines of the frequency patterns with minimum flare contribution. The pre-slit was again used to check that the optical path was clear and then tracing was begun.

The KODAK SO 278 Film diffuse vs. microdensitometer density data plotted in Figure 2.6-1 are given in Table A-.. The Kodak test-target grey step numbers are given in Figure 2.1-1 of the text.

TABLE A-1 MICRODENSITOMETER DENSITY DATA

Grey Step Number	Diffuse (Macbeth) Density	Microdensitometer Density
1	1.55	1.83
2	1.42	1.66
3	1.26	1.49
4	1.09	1.28
5	0.95	1.12
6	0.93	1.13
7	0.77	0.88
8	0.63	0.71
9	0.49	0.53
10	1.51	1.78

APPENDIX B

SMALL-SCALE IMAGE CHARACTERISTIC CURVES

The ANSCO-4 microdensitometer was used to obtain small-scale image D-Log E curves (see para. 2.2 text). The frequency patterns for the Kodak sinusoidal test target and its images were traced. The Kodak target serves as a sensitometric tablet. Dividers were used to obtain the Log E (target density) value corresponding to an image density. Using this method, one data point can be obtained each half cycle (see Figure B-1). Due to great change in density that result in the iamge density for a small change in the target density it was decided to select fixed image densities and find corresponding target densities. Normally it would be expected to obtain image densities corresponding to fixed target densities. The results obtained are repeatable. An example is given in Table B-1.

TABLE B-1 REPEATABILITY: TRACES MADE OF IMAGE Nr 32b, A 12 CYCLE/MM PATTERN

	Corresponding Target Density Using Trace No.					
Image Density	#1	#2	#3	#4	#5	#6
4.00	0.80	0.79	0.81	0.80	0.80	0.78
3.80	0.81	0.80	0.83	0.82	0.81	0.81
3.60	0.85	0.81	0.90	0.88	0.85	0.82
3.00	0.93	0.87	0.99	0.97	0.94	0.92
2.00	1.02	1.02	1.06	1.06	1.04	1.02
1.00	1.13	1.10	1.18	1.15	1.16	1.12
0.70	1.19	1.18	1.20	1.19	1.19	1.18
0.40	1.21	1.20	1.22	1.21	1.21	1.21
0.30	1.22	1.22	1.25	1.22	1.23	1.22
0.20	1.25	1.26	1.29	1.26	1.29	1.26

Note: Six image traces and one target trace were used.

The repeatability of the iamge traces, having been established, it was decided to use one trace of the image, using more than one cycle to obtain a mean log E (target density) value. A reliable Log E was needed in order to minimize the error in the position of the various small- image characteristic curves along the X axis.

This error occurs because the microdensitometer must be refocused and rezeroed at each frequency pattern. The manner in which the target density for a fixed image density of 3.5 was obtained from the 3/8 cycle/mm pattern, trace No. 1 is illustrated (see Figure B-1 and Table B-1). Table B-1 is the microdensitometer data obtained from Negative 65b at three spatial frequencies. Similar data were obtained from the other negatives and composited as image densities and average target densities in Table B-2 (infectious) and B-3 (noninfectious). See text Table e.4-1 for development conditions. The microdensitometer densities in Tables B-2 and B-3 were converted to diffuse densities using the relationship given in the text (see Figure 2.6-1).

FIGURE B-1 Example of Fixed Image Density Value, 3.5, Being Used to Obtain Corresponding Target Density Values.

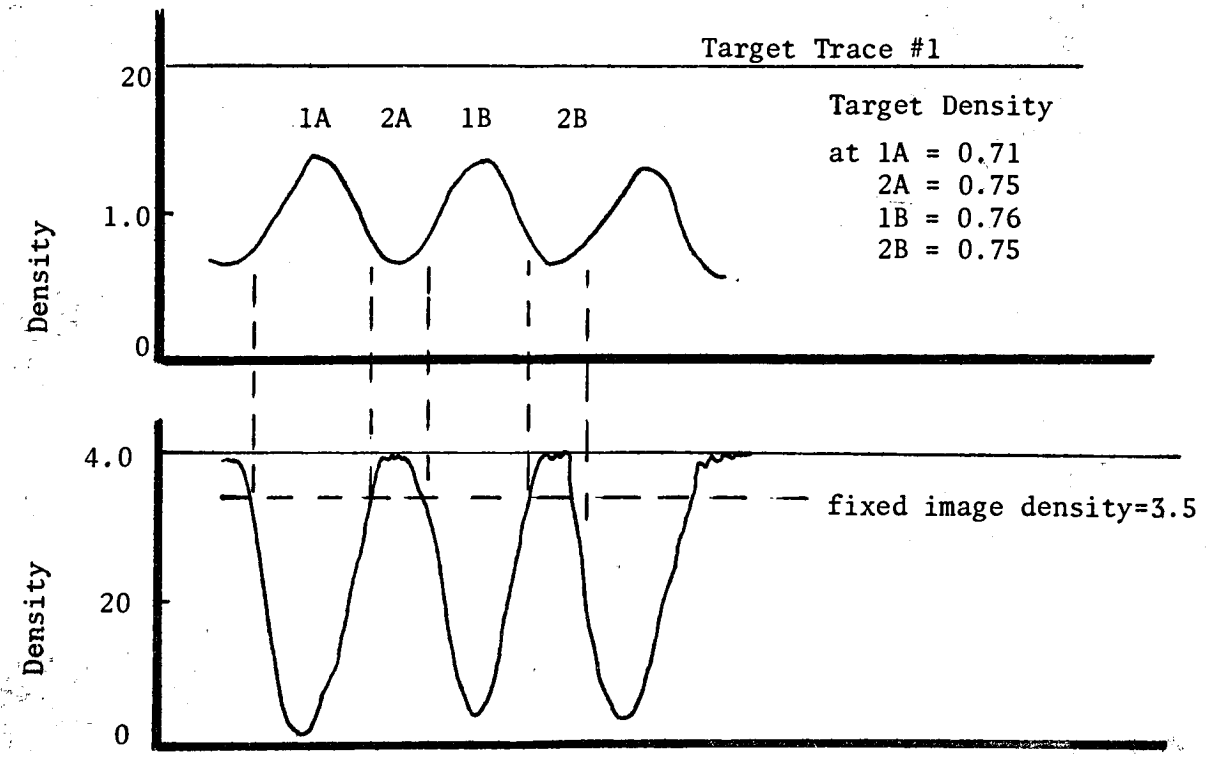

APPENDIX B

Log Exposure (target density) values corresponding to fixed image densities (Neg. 65b) obtained from microdensitometer traces.

TABLE B-1

Neg 65b Image Density	1/2 Cycle	3/8 cycles/mm Target Traces #1	#2	#3	#4	Avg Tgt Density	3 cycles/mm Target Traces #1	#2	#3	#4	Avg Tgt Density	6 cycles/mm Target Traces #1	#2	#3	#4	Avg Tgt Density
3.5	1A	0.71	0.73	0.75	0.75	0.75	0.76	0.76	0.73	0.79	0.78	0.77	0.80	0.79	0.78	0.78
	2A	0.75	0.73	0.76	0.75		0.78	0.80	0.79	0.79		0.75	0.77	0.80	0.78	
	1B	0.76	0.74	0.75	0.73		0.80	0.77	0.81	0.79		0.78	0.76	0.78	0.77	
	2B	0.75	0.73	0.76	0.77											
2.5	1A	0.72	0.74	0.76	0.76	0.78	0.84	0.83	0.77	0.83	0.84	0.83	0.83	0.84	0.83	0.83
	2A	0.78	0.77	0.78	0.79		0.85	0.85	0.85	0.86		0.84	0.80	0.81	0.84	
	1B	0.79	0.78	0.79	0.80		0.84	0.83	0.84	0.83		0.86	0.82	0.84	0.84	
	2B															
2.0	1A	0.77	0.80	0.80	0.83	0.81	0.86	0.84	0.80	0.85	0.85	0.82	0.85	0.85	0.85	0.86
	2A	0.80	0.80	0.82	0.83		0.85	0.85	0.86	0.87		0.87	0.87	0.83	0.87	
	1B	0.79	0.79	0.80	0.82		0.85	0.84	0.85	0.88		0.87	0.86	0.87	0.86	
	2B	0.80	0.79	0.83	0.83											
1.5	1A	0.79	0.82	0.83	0.85	0.82	0.87	0.85	0.84	0.86	0.87	0.85	0.86	0.87	0.87	0.87
	2A	0.80	0.82	0.83	0.85		0.86	0.87	0.86	0.89		0.88	0.88	0.90	0.88	
	1B	0.80	0.80	0.82	0.83		0.86	0.84	0.94	0.88		0.87	0.87	0.87	0.88	
	2B	0.82	0.80	0.84	0.85											
0.9	1A	0.81	0.84	0.84	0.87	0.84	0.89	0.89	0.92	0.88	0.89	0.93	0.89	0.90	0.90	0.90
	2A	0.81	0.83	0.85	0.87		0.88	0.91	0.90	0.90		0.93	0.92	0.90	0.91	
	1B	0.84	0.83	0.85	0.85		0.90	0.85	0.86	0.90		0.91	0.89	0.89	0.89	
	2B	0.84	0.81	0.86	0.85											

Neg. 65b Image Density	1/2 Cycle	3/8 cycles/mm Target Traces #1	#2	#3	#4	Avg Tgt Density	3 cycles/mm Target Traces #1	#2	#3	#4	Avg Tgt Density	6 cycles/mm Target Traces #1	#2	#3	#4	Avg Tgt Density
0.4	1A	0.85	0.89	0.86	0.92	0.88	0.92	0.93	0.88	0.94	0.92	0.94	0.92	0.96	0.92	0.93
	2A	0.85	0.85	0.88	0.90		0.92	0.92	0.93	0.94		0.95	0.92	0.96	0.92	
	1B	0.87	0.87	0.89	0.90		0.92	0.93	0.93	0.90		0.95	0.92	0.91	0.91	
0.2	1A	0.88	0.92	0.92	0.95	0.93	0.95	0.94	0.90	0.96	0.94	0.96	0.97	0.98	0.94	0.97
	2A	0.90	0.92	0.95	0.95		0.95	0.97	0.94	0.95		0.97	0.99	1.02	0.98	
	1B	0.92	0.93	0.93	0.94		0.95	0.92	0.93	0.94		0.96	0.96	0.96	0.97	
0.1	1A	0.93	0.98	1.01	1.01	1.00	1.02	1.03	0.97	1.03	1.04	1.06	1.04	1.07	1.03	1.05
	2A	0.95	0.98	1.01	1.01		1.02	1.04	1.00	1.04		1.06	1.09	1.10	1.08	
	1B	1.01	1.01	1.02	1.03		1.02	0.98	1.03	1.04		1.02	1.02	1.04	1.04	
0.05	1A	1.03	1.05	1.05	1.08	1.05	1.12	1.10	1.14	1.15	1.14	1.13	1.14	1.13	1.10	1.12
	2B						1.13	1.14	1.10	1.16		1.05	1.15	1.16	1.15	

TABLE B-2

MICRODENSITOMETER IMAGE DENSITIES AND

AVG. LOG E (TARGET DENSITIES) FOR INFECTIOUS DEVELOPMENT

INFECTIOUS DEVELOPMENT

MICRODENSITOMETER DENSITIES

Neg 65b Image Density	Average Target Density at the spatial frequencies (cycles/mm) of 3/8	3	6	9	12	15
3.50	0.75	0.78	0.78	0.75	0.74	0.78
2.50	0.78	0.84	0.83	0.81	0.81	0.84
2.00	0.81	0.85	0.86	0.82	0.84	0.86
1.50	0.82	0.87	0.87	0.84	0.86	0.88
0.90	0.84	0.89	0.90	0.89	0.89	0.93
0.40	0.88	0.92	0.93	0.94	0.95	1.00
0.20	0.93	0.94	0.97	0.98	1.01	1.06
0.10	1.00	1.04	1.05	1.03	1.08	1.15
0.05	1.05	1.14	1.12	1.14	1.18	1.35
Neg 65c Image Density	**3/8**	**3**	**6**	**9**	**12**	**15**
3.50	0.84	0.88	0.90	0.85	0.79	0.84
2.50	0.89	0.91	0.95	0.92	0.89	0.90
2.00	0.91	0.92	0.98	0.94	0.94	0.96
1.50	0.92	0.94	1.00	0.96	1.00	1.00
0.90	0.96	0.97	1.05	1.02	1.04	1.06
0.20	1.01	1.06	1.12	1.12	1.14	1.20
0.10	1.08	1.14	1.20	1.14	1.20	1.25
0.05	1.14	1.19	1.31	1.20	1.26	1.30
Neg 65d Image Density	**3/8**	**3**	**6**	**9**	**12**	**15**
3.90	0.88					
3.50	0.92	0.94	0.93	0.94	0.89	0.85
3.00	0.94	0.96	0.97	1.00	0.96	0.92
2.50	0.95	0.99	1.02	1.04	1.02	0.99
2.00	0.98	1.00	1.04	1.08	1.06	1.09
1.50			1.08			
0.90	1.01	1.04	1.11	1.15	1.16	1.20
0.20	1.10	1.11	1.22	1.24	1.30	1.30
0.10	1.18	1.16	1.28	1.30	1.32	1.38
0.05	1.25	1.26	1.32			

NON INFECTIOUS DEVELOPMENT

MICRODENSITOMETER DENSITY

TABLE B-3

Neg 65x Image Density	Average Target Density at the Spatial Frequencies (cycles/mm) of 3/8	3	6	9	12	15
2.50			0.75			
2.00	0.74	0.71	0.81			
1.90						0.76
1.50	0.79	0.83	0.84	0.76	0.78	0.81
0.90	0.89	0.90	0.93	0.87	0.82	0.89
0.40	0.97	1.00	1.03	0.96	0.93	1.00
0.20	1.07	1.07	1.11	1.02	1.03	1.10
0.10	1.15	1.15	1.23	1.18	1.12	1.22
0.05	1.25	1.24	1.28	1.30	1.38	1.40

Neg 65v Image Density	3/8	3	6	9	12	15
3.00			0.76			
2.50	0.70	0.74	0.80		0.74	
2.40						0.77
2.20				0.75		
2.00	0.75	0.79	0.85		0.79	0.80
1.50	0.82	0.84	0.90	0.84	0.83	0.85
0.90	0.91	0.93	0.97	0.91	0.90	0.91
0.40	0.98	1.02	1.08	1.00	1.03	1.01
0.20	1.10	1.08	1.17	1.11	1.11	1.12
0.10	1.17	1.25	1.28	1.22	1.26	1.23
0.05	1.25	1.3]	1.36	1.29	1.42	1.34

Neg 65z Image Density	3/8	3	6	9	12	15
3.50	0.72	0.77	0.75	0.78	0.79	
3.40						0.77
3.00	0.77	0.84	0.83	0.83	0.82	0.83
2.50	0.85	0.90	0.86	0.88	0.85	0.87
2.00	0.92	0.94	0.94	0.94	0.92	0.92
1.50	1.00	1.01	1.01	1.01	0.99	1.00
0.90	1.09	1.10	1.09	1.09	1.07	1.07
0.40	1.20	1.21	1.18	1.19	1.19	1.20
0.20	1.26	1.29	1.26	1.25	1.27	1.28
0.10	1.33	1.37	1.35	1.32	1.36	1.35
0.05	1.41	1.52	1.41	1.40	1.50	----

TABLE B-4

DIFFUSE IMAGE & TARGET DENSITIES FOR INFECTIOUS DEVELOPMENT

Neg 65 b Image Density		Average Target at the Spatial frequencies(cycl				
	3/8	3	6	9	12	15
2.72	0.59	0.61	0.61	0.59	0.58	0.61
1.94	0.61	0.66	0.65	0.63	0.63	0.66
1.56	0.63	0.67	0.68	0.64	0.67	0.68
1.17	0.64	0.68	0.68	0.66	0.68	0.69
* 0.70	0.66	0.70	0.70	0.70	0.70	0.73 *
0.34	0.69	0.72	0.73	0.74	0.74	0.78
0.18	0.73	0.74	0.76	0.77	0.80	0.83
0.10	0.78	0.82	0.82	0.81	0.84	0.90
0.05	0.82	0.89	0.88	0.89	0.92	1.05

Neg 65c Image Density						
	3/8	3	6	9	12	15
2.72	0.66	0.69	0.70	0.67	0.62	0.66
1.94	0.70	0.71	0.74	0.72	0.70	0.70
1.56	0.71	0.72	0.77	0.74	0.74	0.75
1.17	0.72	0.74	0.78	0.75	0.78	0.78
* 0.70	0.75	0.76	0.82	0.80	0.82	0.83 *
0.18	0.80	0.83	0.88	0.88	0.89	0.94
0.10	0.84	0.89	0.94	0.89	0.94	0.98
0.05	0.89	0.93	1.02	0.94	0.98	1.02

Neg 65d Image Density						
	3/8	3 **	6	9 **	12	15 **
3.04	0.69					
2.72	0.72	0.74	0.73	0.74	0.70	.67
2.34	0.74	0.75	0.76	0.78	0.75	.72
1.94	0.74	0.77	0.80	0.82	0.80	0.77
1.56	0.77	0.78	0.82	0.84	0.83	0.85
1.17	-	-	0.84	-	-	-
* 0.70	0.80	0.82	0.87	0.90	0.91	0.94 *
0.18	0.86	0.87	0.95	0.97	1.02	1.02
0.10	0.92	0.91	1.00	1.02	1.03	1.08
0.05	0.98	0.98	1.03			

* The speed values in Figure 3.1-2A are the average of target densities (averaged after 0.09 added - Neg 65c and 0.17 added - Neg 65a)

** These three spatial frequency D - Log E curves plotted in Figure 3.1-1

TABLE B-5

DIFFUSE IMAGE & TARGET DENSITY FOR

NON INFECTIOUS DEVELOPMENT

Neg 65W Image Density	Average Target Density at the Spatial Frequencies (cycles/mm) of 3/8	3	6	9	12	15
1.94			0.59			
1.56	0.58	0.56	0.63			
1.48						0.60
1.17	0.62	0.65	0.66	0.60	0.61	0.63
*0.70	0.70	0.70	0.73	0.68	0.64	0.70*
0.34	0.76	0.78	0.81	0.75	0.73	0.78
0.18	0.84	0.84	0.87	0.80	0.81	0.86
0.10	0.90	0.90	0.96	0.92	0.88	0.95
0.05	0.98	0.97	1.00	1.02	1.08	1.09

Neg 65x Image Density	3/8	3	6	9	12	15
2.34			0.60			
1.94	0.55	0,58	0.63		0.58	
1.86						0.60
1.71				0.59		
1.56	0.59	0.62	0.67		0.62	0.63
1.17	0.64	0.66	0.70	0.66	0.64	0.67
*0.70	0.71	0.73	0.76	0.71	0.70	0.71*
0.34	0.77	0.80	0.84	0.78	0.81	0.79
0.18	0.86	0.84	0.91	0.87	0.87	0.88
0.10	0.92	0.98	1.00	0.95	0.98	0.96
0.05	0.98	1.03	1.06	1.01	1.11	1.04

Neg 65z Image Density	3/8	3**	6	9**	12	15**
2.72	0.56	0.60	0.59	0.61	0.62	
2.64						0.60
2.34	0.60	0.66	0.64	0.64	0.64	0.65
1.94	0.67	0.70	0.68	0.69	0.67	0.68
1.56	0.72	0.74	0.74	0.74	0.72	0.72
1.17	0.78	0.79	0.79	0.79	0.77	0.78
*0.70	0.85	0.86	0.85	0.85	0.84	0.84*
0.34	0.94	0.95	0.92	0.93	0.93	0.94
0.18	0.98	1.01	0.98	0.97	0.99	1.00
0.10	1.04	1.07	1.05	1.03	1.06	1.05
0.05	1.10	1.18	1.10	1.09	1.23	

* Speed values in Figure 3.1-2B are avg. of target densities (averaged after 0.09 added to Neg 65x and 0.17 to Neg 65w).

** D-Log E curves plotted in Figure 3.2-1

APPENDIX C

The grey scale of the sinusoidal test target (Figure 2.1-1) and KODALITH images were used to obtain the large image area D-Log E curves. With one image there were few points obtained on the straight-line portion because the contrast was so high. D-Log E curves with different points along the straight line portion were obtained by varying the exposure time and leaving the source intensity constant. The D-Log E curves, whose position along the target density axis differed by the Log difference in exposure time were superimposed. The superposition corresponded to the interchanging of time with intensity (through the target). There was no reciprocity at the times used (see Figure 2.5-1, text). The result were D-Log E curves with increased number of points along the straight line portion.

The infectious and noninfectious D-Log E data are given in Table 1C. (See para. 2.3 for development conditions). The density values in Table 1C are average of duplicate reading made on the Macbeth TD 102 densitometer (yellow filter).

TABLE 1C

KODALITH Target Image #	Density infectious development				Density noninfectious development				Density of Sinusoidal Test Target or (Log E axis)
	65a	65b	65c	65d	65w	65x	65y	65z	
Exposure Time (sec)	2.5	3.0	3.6	4.4	2.5	3.0	3.6	4.4	
Grey Scale Step #1	0.04	0.04	0.04	0.04	0.04	0.04	0.04	0.04	1.55
2	0.04	0.04	0.04	0.04	0.04	0.04	0.04	0.05	1.42
3	0.04	0.04	0.04	0.05	0.04	0.04	0.05	0.07	1.26
4	0.04	0.05	0.07	0.11	0.06	0.06	0.08	0.18	1.09
5	0.06	0.09	0.14	0.65	0.09	0.16	0.22	0.65	0.95
6	0.08	0.09	0.17	0.41	0.10	0.17	0.30	0.59	0.93
7	0.14	0.29	1.58	2.61	0.33	0.64	1.02	1.64	0.77
8	0.84	2.30	3.57	4.0+	1.09	1.35	1.86	2.53	0.63
9	3.17	4.0+	4.0+	4.0+	1.80	2.06	2.84	3.29	0.49
10	0.04	0.04	0.04	0.04	0.04	0.04	0.04	0.04	1.51

The data as arranged in Table 2C were used in Figure 2.7-1 (with 0.04 base + fog density added to the image and target values) and in Figures 3.1-1 and 3.2-2. The D-Log E curves were superimposed so that they could be plotted with negatives having 4.4 sec exposure. The shifts made were the Log exposure difference between the 4.4 sec negatives and the other negatives (see Table 2.4.1 text).

The confidence intervals for the speed (at 0.70 density and the curve gradient can be obtained by regression of the straight line portion of the D-Log E curve using method in Chapter 12 of STATISTIC AN INTRODUCTION by Rickmers & Todd, McGraw-Hill Book Co., 1967.

TABLE C-2

INFECTIOUS DEVELOPMENT

Image # & Step #	Net Image Density	Net Target Density
65c 8	3.53	0.68 ***
65a 9	3.13	.70 *
65d 7	2.57	.73
65b 8	2.26	.76 **
65c 7	1.54	.82 ***
65a 8	0.80	.84 *
65d 5	0.61	.91
65d 6	0.37	.89
65b 7	0.25	.92 **
65c 6	0.13	.98 ***
65a 7	0.10	.98 *
65c 5	0.10	1.00 ***
65d 4	0.07	1.05
65b 5	0.05	1.07 **
65b 6	0.05	1.06 **
65a 6	0.04	1.14 *
65c 4	0.03	1.14 ***
65d 3	0.01	1.22

"NON INFECTION" DEVELOPMENT

Image # & Step #	Net Image Density	Net Target Density
65z 9	3.25	.45
65y 9	2.80	.54 ***
65z 8	2.49	.59
65x 9	2.02	.62 **
65y 8	1.82	.68 ***
65w 9	1.76	.70 *
65z 7	1.60	.73
65x 8	1.31	.76 **
65w 8	1.05	.84 *
65y 7	.98	.82 ***
65z 5	.61	.91
65x 7	.60	.90 **
65z 6	.55	.89
65w 7	.29	.98 *
65y 6	.26	.98 ***
65y 5	.18	1.00 ***
65z 4	.14	1.05
65x 6	.13	1.06 **
65x 5	.12	1.08 **
65w 6	.06	1.14 *
65w 5	.05	1.16 *
65y 4	.04	1.14 ***
65z 3	.02	1.22
65x 4	.02	1.22 **
65w 4	.02	1.30 *
65y 3	.01	1.31 ***
65z 2	.01	1.38

Target density shifted by

* +0.25
** +0.17
*** =0.09

See Figure 2.7-1
Infectious D-Log E See Figure 3.1-1
"Non Infect. D-Log E See Figure 3.2-1

APPENDIX D

DATA USED IN FIGURES 2.7-1 AND 2.8-1

"TEST STRIPS"-KODALITH SUPER DEVELOPER"

Large-Image-Area-Characteristic Curve obtained from test strips of varying log exposures. KODALITH type 3 film strips exposed in a 101 sensitometer with a 1700 mc source intensity. Density of step wedge in the sensitometer given below. Strip 15 a was exposed for 0.2 sec for a total of 2.53 mcs. Strip 15 b was exposed for 0.4 sec for a total of 2.83 mcs. A Macbeth densitometer, model TD102 was used for density readings. KODALITH Super Developer was used at 68 F for 2 minutes, 45 seconds.

TABLE D-1

Density Step Wedge in sensitometer	Strip 15a Log E	Strip 15a Macbeth Density	Strip 15b Log E	Strip 15b Macbeth Density
0.04	-	-	-	-
0.18	-	-	-	-
0.34	-	-	-	-
0.50	-	-	-	-
0.65	-	-	-	-
0.81	1.72	3.30	-	-
0.95	1.58	1.22	-	4.00
1.09	1.44	0.19	1.74	3.11
1.24	1.29	0.08	1.59	1.20
1.41	1.12	0.05	1.42	0.17
1.55	0.98	0.04	1.28	0.08
1.61	0.92	0.04	1.22	0.06
1.83	0.70	0.04	1.00	0.04
1.97	0.56	-	-	-
2.14	-	-	-	-
2.30	-	-	-	-
2.45				
2.57				
2.72				
2.92				
3.08				

APPENDIX D

DATA USED IN FIGURE 2.8-1

KODALITH SUPER DEVELOPER PLUS 20 g/1 Na_2SO_3

Large-Image-Area Characteristic curve from test strips - KODALITH Type-3 Film exposed in 101 sensitometer (1700 mc source intensity) for 0.2 sec for total exposure of 2.53 mcs. Step wedge in sensitometer has densitites listed below. Density reading were made with Macbeth instrument. KODALITH Super Developer plus 20 g/liter of sodium sulfite were used at 68 F for 2 minutes, 45 seconds.

TABLE D-2

Density Step Wedge in Sensitometer	Absicissa Log E	Strip 40 a density	Strip 40 b density	Average density (Ordinate)
0.04	--	--	--	--
0.18	--	--	--	--
0.34	2.19	4.00	4.00	4.00
0.50	2.03	3.54	3.46	3.50
0.65	1.88	2.80	2.76	2.79
0.81	1.72	2.04	2.17	2.11
0.95	1.58	1.36	1.45	1.40
1.09	1.44	0.64	0.74	0.69
1.24	1.29	0.23	0.30	0.27
1.41	1.12	0.10	0.11	0.11
1.55	0.98	0.06	0.06	0.06
1.61	0.92	0.04	0.04	0.04
1.83	--	--	--	--
1.97	--	--	--	--
2.14	--	--	--	--
2.30	--			
2.45	--			
2.57	--			
2.72	--			
2.92	--			
3.08	--			

APPENDIX D

DATA USED IN FIGURE 2.8-1

KODALITH SUPER DEVELOPER PLUS 50 g/1 Na_2SO_3

Large Image Area Characteristic curve from test strips - KODALITH Type-3 Film exposed in 101 sensitometer (1700 mc source intensity) for 0.2 sec for total exposure of 2.53 mcs. Step wedge in sensitometer has densities listed below. Density readings were made with a Macbeth instrument. KODALITH Super Developer plus 50 g/1 of sodium sulfite were used at 68 F for 2 minutes, 45 seconds.

TABLE D-3

Density Step Wedge in sensitometer	Abscissa Log E	Strip 42a Density	Strip 42b Density	Ordinate Average Density
0.04	2.49	4.00	4.00	4.00
0.18	2.35	3.86	3.84	3.85
0.34	2.19	3.27	3.30	3.28
0.50	2.03	3.78	2.92	2.85
0.65	1.88	2.28	2.34	2.31
0.81	1.72	1.74	1.74	1.74
0.95	1.58	1.22	1.22	1.22
1.09	1.44	0.74	0.68	0.71
1.24	1.29	0.36	0.35	0.35
1.41	1.12	0.16	0.14	0.15
1.55	0.98	0.08	0.07	0.08
1.61	0.92	0.04	0.05	0.05
1.83	0.70	0.04	0.04	0.04
1.97	0.56	0.04	0.04	0.04
2.14	-	0.04	0.04	0.04
2.30	-			
2.45	-			
2.57	-			
2.72	-			
2.92	-			
3.08	-			

APPENDIX E

The average gradient meter (see Figure 2.5-1, text) is an ellipse made by drawing two circles, one of which has the radius of the y axis and the other the radius of the x axis. The y axis radius was selected to be 2.3 units since average gradients are commonly taken between densities of 0.2 and approximately 2.5 (2.3 units). The x axis radius was selected on the basis of the latitude of the films used. As is seen in the diagram (see Figure E-1) the abscissa of a point is found where OA intersects the small circle.

The ordinate is found by drawing a line AB parallel to OZ. Another OA line is selected and a new point found on the ellipse. Upon completion of the ellipse the position of lines of given slopes are used to calibrate the gradient meter. It is then made into a transparency and used. The average gradient found using the meter is equal to (D_2-D_1) / (Log E_2-Log E_1) where D_1 = 0.2 above base + fog and D_2 is the intersection of the L-Log E curve with the ellipse. This average gradient meter has the advantage of giving gradinets with a normal distribution rather than a bimodal one as some gradient meters have done. For example, the meter shown below has average gradients measured between D_1 and an index density D_2 if the crossover point is between D_2 and X. If the crossover occurs between X and E_X the average gradient is measured at the density between E_X and X divided by log E_X.

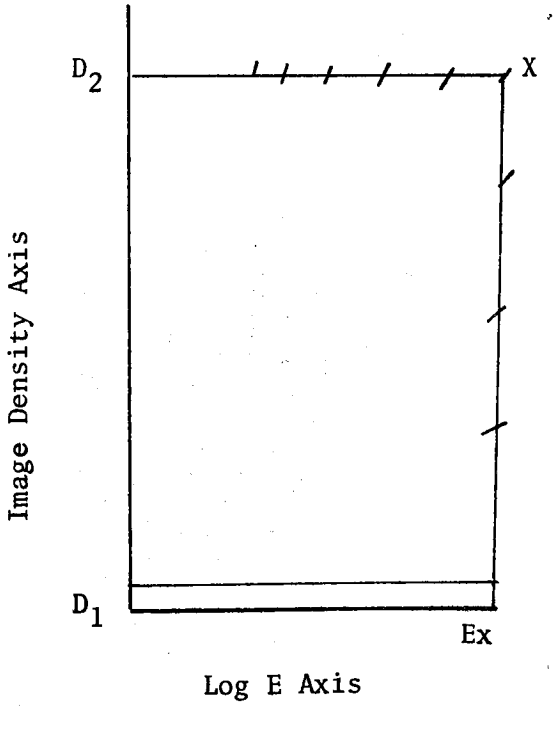

Figure E-1

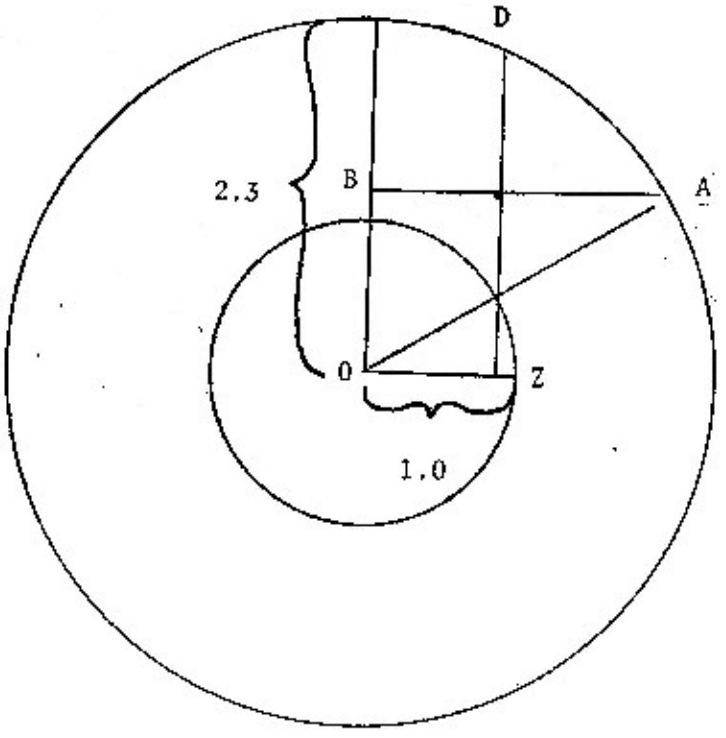

Figure E.1

APPENDIX E

TABLE E-1

INFECTIOUS DEVELOPMENT - AVERAGE GRADIENTS

Spatial Freq.	LIA	3/8	3	6	9	12	15
Neg 65b		18	20	16	13	10	10
Neg 65 c		19	17	14	12	8.5	8
Neg 65d		17	18	13	11	8	7
Neg's *65b, 65c & 65d	11						
**101 SensiStrips	10						
Average	10.5	18	18.3	14.3	12	8.8	8.3
***$A_{\bar{x}}$	.42	.69	1.05	1.05	.69	.72	1.05
$2A_{\bar{x}}$	.8	1.4	1.1	2.1	1.4	1.4	2.1

* Appendix C Table C-2, D-Log E data.

** Appendix D p1, D-Log E data

*** $A_{\bar{x}} = \sqrt{\frac{\Sigma(X - \bar{X})^2}{\eta(\eta-1)}}$

η = observations

$\bar{X}$ = average of observed points

APPENDIX E

TABLE E-2

NONINFECTIOUS DEVELOPMENT

Spatial Freq.	LIA	3/8	3	6	9	12	15
Neg. 65x		6.5	6.5	6.0	6.6	6.0	6.5
Neg 65y		6.5	7.0	7.0	6.7	6.5	7.0
Neg. 65z		5.5	5.7	6.0	6.4	6.0	6.0
Negs *65x, 65y & 65z	4.7						
**101 SensiStrips	3.7						
Average	4.2	6.2	6.4	6.3	6.6	6.2	6.5
$A_{\bar{x}}$		.42	.40	.45	.4	.11	.2	.34
$2A_{\bar{x}}$		.8	.8	.9	.8	.2	.2	.7

* Appendix C, Table C-2, D-Log E data.

** Appendix D, p-2, D-Log E data.

$$A_{\bar{x}} = \sqrt{\frac{\Sigma(X-\bar{X})^2}{(n-1)n}}$$